energies

MDPI

Review

Triboelectric Nanogenerators for Energy Harvesting in Ocean: A Review on Application and Hybridization

Ali Matin Nazar [1], King-James Idala Egbe [1], Azam Abdollahi [2] and Mohammad Amin Hariri-Ardebili [3,4,*]

[1] Institute of Port, Coastal and Offshore Engineering, Ocean College, Zhejiang University, Zhoushan 316021, China; ali.matinnazar@zju.edu.cn (A.M.N.); ekjames@zju.edu.cn (K.-J.I.E.)
[2] Department of Civil Engineering, University of Sistan and Baluchestan, Zahedan 45845, Iran; azam.abdollahi@pgs.usb.ac.ir
[3] Department of Civil Environmental and Architectural Engineering, University of Colorado, Boulder, CO 80309, USA
[4] College of Computer, Mathematical and Natural Sciences, University of Maryland, College Park, MD 20742, USA
* Correspondence: mohammad.haririardebili@colorado.edu; Tel.: +1-303-990-2451

Abstract: With recent advancements in technology, energy storage for gadgets and sensors has become a challenging task. Among several alternatives, the triboelectric nanogenerators (TENG) have been recognized as one of the most reliable methods to cure conventional battery innovation's inadequacies. A TENG transfers mechanical energy from the surrounding environment into power. Natural energy resources can empower TENGs to create a clean and conveyed energy network, which can finally facilitate the development of different remote gadgets. In this review paper, TENGs targeting various environmental energy resources are systematically summarized. First, a brief introduction is given to the ocean waves' principles, as well as the conventional energy harvesting devices. Next, different TENG systems are discussed in details. Furthermore, hybridization of TENGs with other energy innovations such as solar cells, electromagnetic generators, piezoelectric nanogenerators and magnetic intensity are investigated as an efficient technique to improve their performance. Advantages and disadvantages of different TENG structures are explored. A high level overview is provided on the connection of TENGs with structural health monitoring, artificial intelligence and the path forward.

Keywords: triboelectric nanogenerators; ocean wave; energy harvesting; artificial intelligence; structural health monitoring

Citation: Matin Nazar, A.; Idala Egbe, K.-J.; Abdollahi, A.; Hariri-Ardebili, M.A. Triboelectric Nanogenerators for Energy Harvesting in Ocean: A Review on Application and Hybridization. *Energies* **2021**, *14*, 5600. https://doi.org/10.3390/en14185600

Academic Editor: Dibin Zhu

Received: 19 July 2021
Accepted: 1 September 2021
Published: 7 September 2021

1. Introduction

Ocean energy is one of the most powerful energy resources in the environment. Waves and tides have a considerable amount of mechanical energy that can be harvested and used toward technological development [1–8]. However, harvesting the ocean's energy is a challenging task because the difference of ions inside the water may damage electronic devices [9]. During the last decade, triboelectric nanogenerators (TENG) have played a remarkable role in ocean energy storage development with numerous benefits [7,8,10]. For example, wind farms have usually been built according to electromagnetism systems and a turbine structure produces environmental noise which is classified as an ecological problem [11–19]. There are several limitations associated with wind farms: They need to be operated under high wind speed, their equipment is very large and the installation price is typically high [20–22]. On the other hand, the TENG can resolve some of the mentioned issues by performing well with lightweight equipment and a low vibration system [23], which allows its application in various situations [24–30]. TENGs have multiple benefits in the context of hybrid energy collection, for instance, the electromagnetism compound with TENG to produce energy based on the ocean waves [31,32]. The principles

of TENG were inspired from triboelectrification [33–36]. Triboelectrification is the process by which two originally uncharged bodies become charged when brought into contact and then separated.

When two dielectric materials are physically in contact and producing a triboelectric charge, a potential difference is generated by dividing two surfaces within the mechanical motion [37–39], making electrons flow in the external circuit and therefore, sets with the electrostatic operation. TENGs can be classified into four modes: Vertical contact separation, lateral sliding, single electrode and freestanding triboelectric layer [31,32,40–49]. Unlike traditional energy harvester devices, which are large [23], costly [50] and complicated to fabricate [51–57], TENGs are low damage and lightweight and they frequently have been applied to create ocean energy power [58,59].

The TENG's principles in ocean energy harvesting can be approximately separated into two stages: (1) Direct contact between the tribo-surface and water and an encapsulated design relying on solid–solid contact [60–77] and (2) direct contact between the tribo-surface and water is like raindrop energy harvesting. The method founded on solid–solid contact is influenced by the surface roughness and the contact/triboelectric field [78,79]. Investigating TENG-based ocean energy harvesting includes various perspectives such as structural design, operation optimization and meteorological regulation [80–97]. Furthermore, the large-scale combination of a TENG network relies on its design for improved flexibility and independence, forming self-powered wireless sensor networks [98–101]. The potential ocean energy utilization includes, but is not restricted to, long-term environmental monitoring, navigation at the ocean, decomposition of the hydrogen fuel water and purification of the polluted water [102]. The TENG networks floating on the ocean shore can be created to combine with another energy harvester [19,103,104].

This review article aims to provide an overview and summarizes the main research trends of TENG in the ocean. Section 2 states an overview of the structure and fundamentals of the ocean and sea waves including some discussion on the advantages and disadvantages of the current energy harvesters. Furthermore, a summary is provided on the physics of TENGs and the parameters that affect its trend. Section 3 introduces the hybridization of TENGs with other types of energy harvester including solar cells and electromagnetic and magnetic intensity. The applications of TENGs and the future challenges are discussed in Section 4 and the paper is concluded with a short summary in Section 5.

2. Fundamentals of Ocean Wave Energy and Different TENG Structures

Devices designed to absorb energy from sea waves are typically installed near shores. This choice of location reduces the risk of damage in stormy conditions [105]. However, due to their proximity to the shore, the amount of generated energy is not significant [106]. The majority of the devices in shallow water are attached to the seabed as a support base. However, their performance is improved if they are installed in deep water. On the other hand, there is an argument about the meaning of "deep" water. Some researchers consider tens of meters to be the definition [107], others say the depth is greater than 40 m [106] and another group take a profundity surpassing one-third of the wavelength [108]. However, all of them are agreed that the energy-absorbing devices from the ocean waves show a supreme performance if they are placed in deep water. The reason is pretty simple: Deep water generates more massive waves and subsequently more energy can be extracted. Nevertheless, it should not be forgotten that access to devices in deep waters is more complicated and the maintenance cost is also high. In addition, since they are located far from the shore and also they are exposed to large waves, it is necessary to consider a special design for them (probably with higher safety factor) [109] which increases the overall cost of the project.

2.1. Global Ocean Wave

A wave farm is a set of wave energy-extracting devices working together in a given location in harmony to produce more energy [110,111]. As a result of their numbers, the re-

gional climate condition and the strategies needed to control them, these devices interact to generate more energy and reduce costs [112–117]. Many companies have invested in this technology and have set up a wave farm in different dimensions over the years [118–122]. Wave characteristics such as wavelengths and velocity at the water surface are fundamental features because they analyze how the waves break on the shores. Several countries including the United States, the United kingdom, Portugal and Australia operate wave farms and kinds of power take-off systems, including elastomeric hose pump, hydraulic ram, pimp-to-shore, hydroelectric turbine, air turbine and linear electrical generator.

2.2. Characteristics of Ocean Wave

The wave energy flux formula is formulated in deep waters where the depth of the water is more than half the wavelength. This equation represents the wave power in terms of the wave energy period, T and the significant wave height, H_{m0}, [123]:

$$P = \frac{\rho g^2}{64\pi} H_{m0}^2 T \tag{1}$$

where P is the wave energy flux per unit of wave-crest length. ρ and g are water density and gravitational acceleration, respectively.

On the other hand, the total potential of an ocean wave can be presented as [124]:

$$E = \frac{1}{2}\rho g A^2 \tag{2}$$

where A is the wave amplitude.

The average energy flux or wave power, P_w, is calculated by multiplying the energy term, E, by wave propagation speed, $V_g = \frac{L}{2T}$. In this formula, T is the wave period and L is the wavelength [125].

$$P_w = \frac{1}{2}\rho g A^2 \frac{L}{2T} \tag{3}$$

The dispersion relationship which describes the connection between the wave period and the wavelength, $L = \frac{gT^2}{2\pi}$, is combined with Equation (3) and results in [125]:

$$P_w = \frac{\rho g^2 T A^2}{8\pi} \quad or \quad P_w = \frac{\rho g^2 T H^2}{32\pi} \tag{4}$$

where H is the wave height.

Wave energy generation is an emerging commercial technology, in comparison with the other renewable energy sources. Since the 1890s, many countries located next to the oceans have been trying to harness this high-potential energy source [126]. In general, the energy harvesting devices from ocean waves can be classified according to their location (including shoreline, nearshore and offshore) and the power take-off system (including hydraulic ram, elastomeric hose pump, pump-to-shore, hydroelectric turbine, air turbine and linear electrical generator) [127]. Similar to other renewable energy sources, the energy from the ocean waves is a significant and endless energy source. While it has been used in many countries like China, the United States, Scotland and Australia, there are several disadvantages associated with this type of energy. Table 1 summarizes the pros and cons of this energy source.

Table 1. Comparing various features related to the wave energy harvesting from the ocean.

Advantage	Disadvantage
Renewable: Unlike fossil fuels, which we see running out every day, the energy from waves is renewable and vast [128]	**Not applicable everywhere:** Just like most natural resources, it is location-specific. Thus, this type of energy is only useful for countries with access to the ocean and sea [128].
Environment Friendly: These days, energy production is a significant problem in the world. On the other hand, pollution from energy production is another concern that human beings pay special attention to because pollution from the production of fossil fuels causes global warming. In contrast, the energy from the waves is environmentally friendly [128].	**Danger to the marine ecosystem:** This type of energy poses a threat to aquatic habitats. Some of these devices fixed to the ocean floor, which can damage habitats and sometimes cause sea creatures to collide with turbine blades or even get electrocuted [129].
Easy access: The advantage of easy access arises for nations with borders along the coast with high wave intensity [128]	**Disruption of ship traffic:** Energy-efficient devices from the ocean waves located near shores and in the direction of the wave, a transit point for cargo ships and cruise ships. These devices make it a bit difficult to get around.
Technology growth in this area: : Many devices have been designed and implemented to extract energy in this [128].	**Poor performance in stormy weather:** One of the problems with wave energy extraction devices is poor performance in rough weather, which can even cause severe damage.
Predictable: One of the essential advantages of this type of energy is calculating the amount of energy production and its predictability.	**Noise pollution:** Another downside of these devices is the noise, which can significantly reduce real estate value for areas near the coast [128].
Less dependence on fossil fuels: It reduces dependence on fossil fuels. It can help reduce pollution around the globe by reducing the dependence on fossil-generated energy [128].	**Dependence on wind:** This wave category is driven by wind, so when the wind is not stable, it is not possible to extract significant energy.
Earth protection: Unlike fossil fuels that require deep drilling for extraction, there is no need to damage the earth to extract this type of energy [130]	

Figure 1a illustrates the absorption point device which works by floating on the water's surface. It is maintained by the cables connected to the seafloor. Generally, the perfect point absorber has the same features as a useful wave-maker. The system of absorption points is ocean-level floating structures whose structural physics is designed to have slightly horizontal dimensions relative to their vertical dimensions. The technology has been hailed by researchers working to obtain energy from ocean waves. When the vessel is excited by the waves (point absorption), it works so that the current moves relative to the fixed reference point. They use linear generators. At the top of this device, the degree of freedom glass considered to create the best necessary performance and also this device use the movement in the heave axis [131–134]. The wave energy converter(WEC) system has three main parts: Buoy, power take-off and heave plate. The buoy part consists of components placed in a series and a vertical direction, the most important hydraulic

cylinder components and a spring. To prevent the device from drowning, the empty volume inside the device is filled with urethane foam. With this method, if water enters the system through the cracks in the device, it will not cause the system to drown. Another innovative feature of this device is that a urethane-shaped ring is attached to the device's outer wall, increasing buoyancy. The power take-off device uses a spring to maintain linear stress. The WEC's hydraulic system also uses four low-pressure valves to control the movement between the inlet and outlet of the end of the cylinder, which is installed at the outlet and before the flow limiter. The primary purpose of this placement is to control the pressure as a function of the current. The heave plate comprises a steel rod fastened to a steel plate. Cast press weights slide over the steel bar, allowing straightforward modification of the common heave plate mass. A parabolic bowl with a center hole slides over the center shaft and clamps onto the barbell weights. The reason for the heave plate is to supply a counter constrain to the buoy.

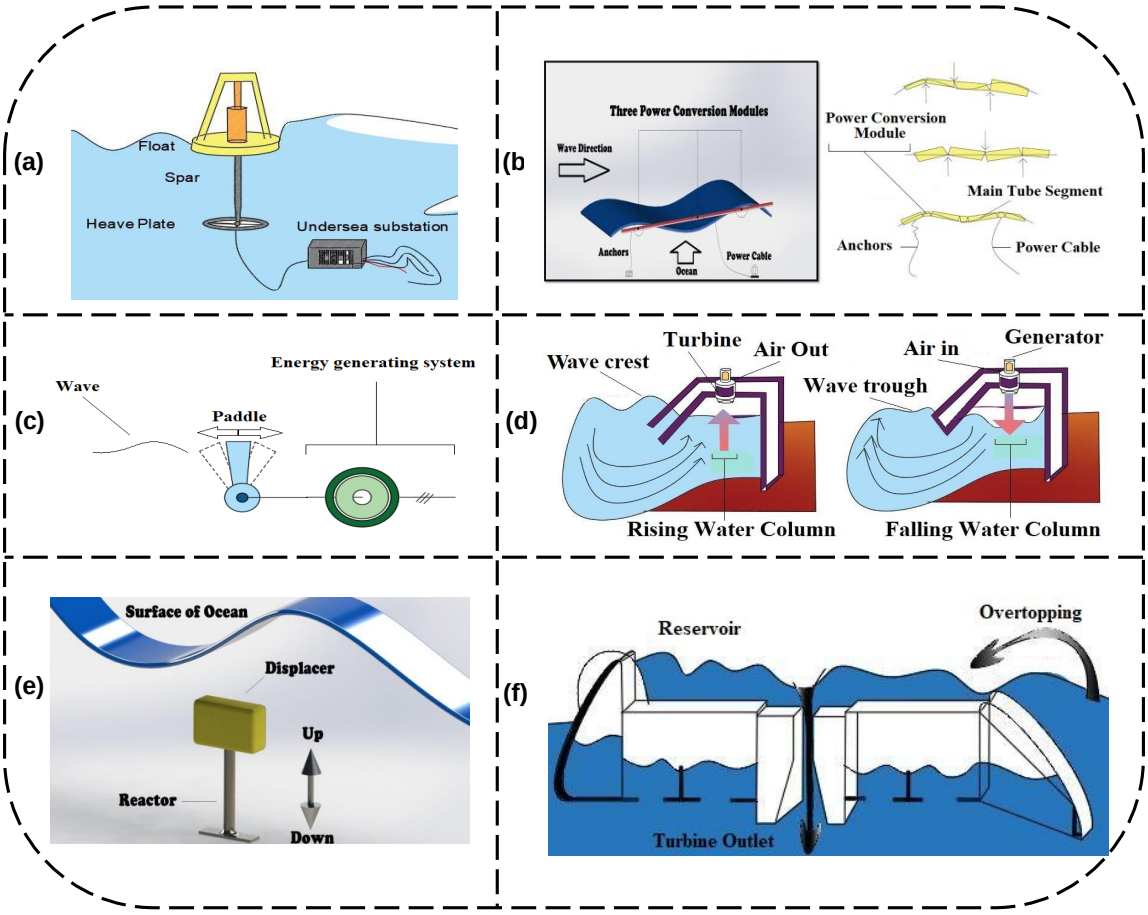

Figure 1. Summary of wave energy converters: (**a**) Point absorber buoy, (**b**) Surface attenuator, (**c**) Oscillating wave surge converter, (**d**) Oscillating water column, (**e**) Submerged pressure differential, (**f**) Overtopping device.

Figure 1b Shows the surface attenuators that are used to convert the energy from ocean waves. They typically move parallel to the ocean waves' direction or parallel to the movement of the ocean waves. In this system, two long pieces are usually connected. The attenuators rely on the flexibility of the joints to produce the power. Examples include surge, sway and heave. One of the most popular and used types of attenuators is WEC Pelamis [134]. Figure 1c demonstrates the oscillating wave surge converter (OWSCs) whose energy is produced using the movement of ocean waves. The structure of this device is made of a central arm or flap, such that, when ocean waves are created, these waves stimulate the designed arm. The flaps are located in a device connected to a generator

and its operation is such that it acts as an arm for a large lever and rotates the generator, which generates electricity or, in other words, converts wave energy into electricity. It is possible. These devices are designed to be used frequently in shallow waters [134–136].

Figure 1d shows the air chamber located at the top of the water surface in the device configuration. In this system when a wave travels across the device, the water level rises and falls with standard performance. The system is designed so that the top of the compartment is a turbine as well as a duct. The primary function of the channel is to enter and exit the air. When the water level in the chamber drops, the pressure in the chamber also decreases, which results in a vacuum. In this case, the air comes from outside the device compartment to the inside. This process occurs back and forth. When the water level rises, excess air escapes from the designed turbine. This water movement puts pressure on the turbine blades, causing them to move and generate electricity [137–140].

Figure 1e presents an overtopping device, also called a stabilizer, that uses the ocean waves to generate energy. The device's function is to simulate the same wave motion seen on the shores and, through that simulation, the electricity generated. The Wave Dragon Project is an example of a conceptual design of an overflow hydraulic power plant. The mechanism of this device's operation is such that the two sloping obstacles are concentrated towards the center of the device. This is to optimize energy harvesting. As a result, spilled water moves the turbine to the center, which is a low-pressure turbine. After that, the spilled water is temporarily stored in a reservoir and returned to the ocean. The system acts as a floating marine power plant not connected to the shore. These types of devices are mostly located near the shores. In order to be most efficient, it adjusts its surface height to the height of the waves that occur in the ocean [141,142].

Figure 1f illustrates submerged pressure differential. This system produces energy based on the differential pressure of immersion in the ocean's depths. It is made up of flexible but amplified membranes to extract energy from ocean waves. The device generally uses the pressure difference under the wave at different locations to create a pressure difference in a liquid system that rises from closed power. This pressure difference directs the turbine, which results in the production of electrical energy. There are two different systems, one located near the coast and on the seabed that relies on pressure fluctuations. The other model is similar to point absorption but immersed in water, which floats back and forth in a wave motion, moving a linear generator to convert energy [143–151].

In summary, Table 2 compares and contrasts the advantages and disadvantages of the six above-discussed modern technologies for energy harvesting from the ocean waves.

Table 2. Comparison of modern technologies used for energy harvesting from ocean waves.

Technology	Advantage	Disadvantage
Point absorber buoy	Simple structure	Habitat destruction
Oscillating wave surge converter	Generates electricity in both forward and reverse directions	Habitat destruction
Submerged pressure differential	Can be used on the seabed and as a float	Danger of electricity for aquatic animals
Surface attenuator	High efficiency	Best performance when it is aligned in the wave direction
Overtopping device	Independence of the beach	Danger of sea animals being trapped in a water storage tank
Oscillating water column	Innovative structure	Danger of turbine blades for aquatic animals

2.3. Physics of Triboelectric Nanogenerators

According to Figure 2, several models have been proposed for the TENGs. The first category is the formal physical model, which is implemented according to the classical electromagnetic theory [152–162]. It should be noted that the 3D mathematical models and the distance-dependent electric field model are created according to the quasi-electrostatic model [141,154–156]. In the second category, an equivalent electrical circuit model is notable. The circuit includes the CA model as well as the Norton equivalent circuit model [153–156].

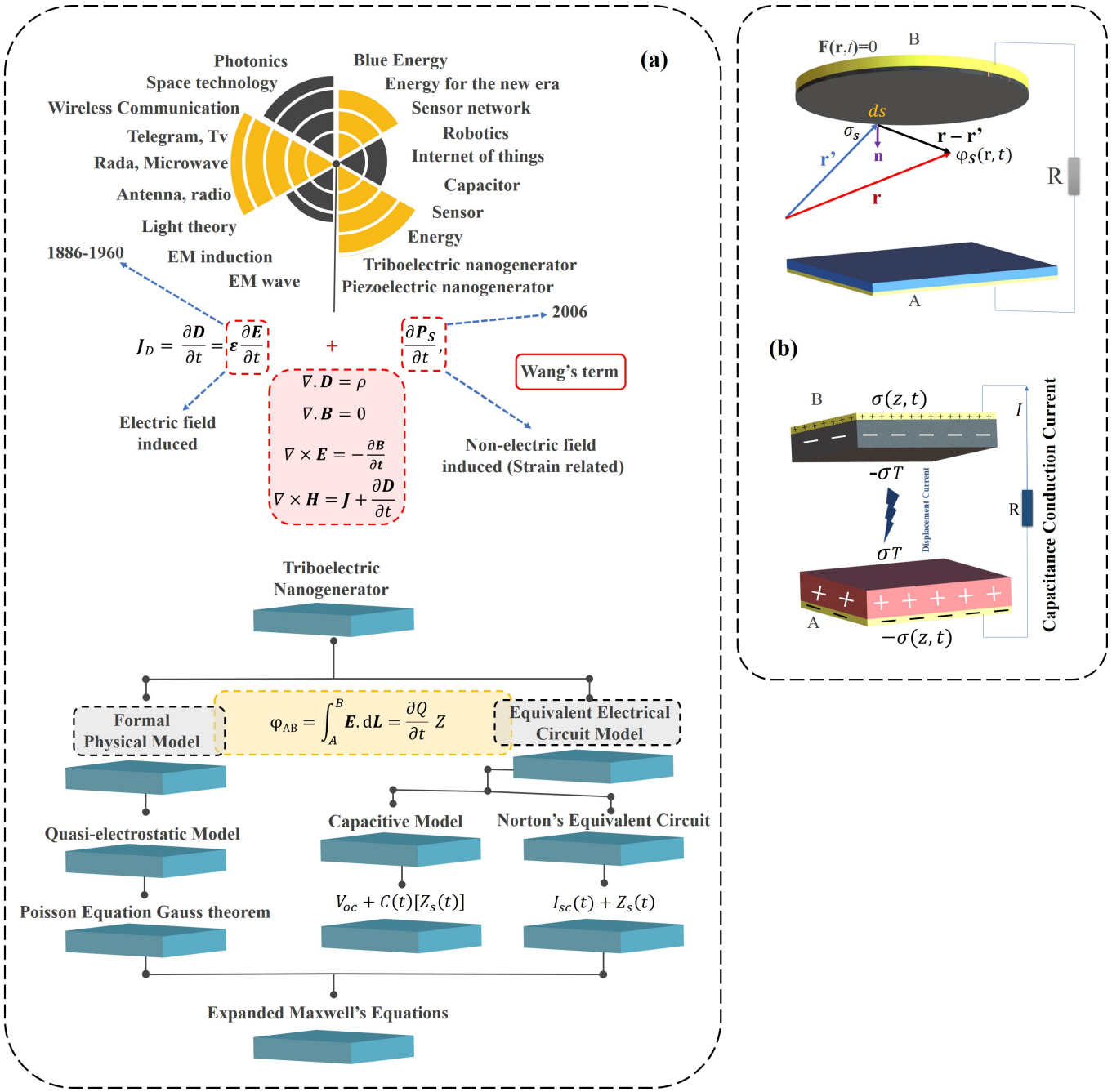

Figure 2. Summary of underpinning theories related to the physics of the TENGs. (**a**) Comparison of displacement current between Maxwell's equation and Wang's expanded equation and relationships between the formal physical model and the equivalent electrical circuit model (TENG models). (**b**) Schematic simulation of nano generator and illustration of a vertical contact-separation mode of TENG.

Figure 2 summarizes a transport equation describing the formal physical model and an equivalent electrical circuit model. It should be noted that both models are linked to each other. As it turns out, ϕ_{AB} is a potential drop for the TENG system which appears in the left side of the equation. Moreover, $V = \frac{\partial Q}{\partial t} \times Z$ presents the voltage across the external load (appearing on the right side). According to Kirchhoff's voltage law, the potential difference between two TENG electrodes is equal to the load resistance voltage. The final product is the transportation equation. The physics of TENGs is determination by the variation of potential, ϕ, electric field, $\boldsymbol{E}$, polarization of the dielectric material, $\boldsymbol{P}$ and the Maxwell's displacement current, $\boldsymbol{I}_D$. The circuit models determine the outputs from the external circuit, e.g., variation of voltage, V, current, I, power P and extracted electrical energy, E [142].

According to Figure 2, Maxwell's equations, known as Wang's term, are added by the term $\boldsymbol{P}_S$ [157]. It should be noted that Wang's term is not the result of moderate polarization due to the $\boldsymbol{P}$ electric field. Wang's term derives from the existence of electrostatic surface charges:

$$\boldsymbol{D} = \varepsilon_0 \boldsymbol{E} + \boldsymbol{P} + \boldsymbol{P}_s \tag{5}$$

The corresponding displacement current density, $\boldsymbol{J}_D$, is given by

$$\boldsymbol{J}_D = \frac{\partial \boldsymbol{D}}{\partial t} = \varepsilon_0 \frac{\partial \boldsymbol{E}}{\partial t} + \frac{\partial \boldsymbol{P}}{\partial t} + \frac{\partial \boldsymbol{P}_s}{\partial t} = \varepsilon \frac{\partial \boldsymbol{E}}{\partial t} + \frac{\partial \boldsymbol{P}_s}{\partial t} \tag{6}$$

where ε_0 and ε are permittivity of free space (vacuum) and permittivity of the material (or medium), respectively. These two terms are connected as $\varepsilon \equiv \varepsilon_0(1 + \gamma_e)$, where γ_e presents the electric susceptibility of the medium. Knowing that $\boldsymbol{P} = (\varepsilon - \varepsilon_0)\boldsymbol{E}$, the volume charge density (Equation (7)) and the density of current density (Equation (8)) are defined by

$$\rho' = \rho - \nabla \cdot \boldsymbol{P}_s \tag{7}$$

$$\boldsymbol{J}' = \boldsymbol{J} + \frac{\partial \boldsymbol{P}_s}{\partial t} \tag{8}$$

Satisfying the charge conversion and continuation equation [157]:

$$\nabla \cdot \boldsymbol{J}' + \frac{\partial \rho'}{\partial t} = 0 \tag{9}$$

As a result, Maxwell's equations are rewritten as [157]:

$$\begin{array}{l} \nabla \cdot \boldsymbol{D}' - \rho' = 0 \\ \nabla \cdot \boldsymbol{B} = 0 \\ \nabla \times \boldsymbol{E} + \frac{\partial \boldsymbol{B}}{\partial t} = 0 \\ \nabla \times \boldsymbol{H} - \boldsymbol{J}' - \frac{\partial \boldsymbol{D}'}{\partial t} = 0 \end{array} \tag{10}$$

It is noteworthy that the self-consistent equations mentioned above describe the relationships between electromagnetic fields and charges as well as the current distribution in TENGs [157], where:

$(\varepsilon \partial \boldsymbol{E}/\partial t)$: Well-known contribution to Maxwell's displacement current.

$(\varepsilon \partial \boldsymbol{P}_s/\partial t)$: Displacement current due to the presence of surface charges

$$\phi_{AB} = \int_A^B \boldsymbol{E} \cdot d\boldsymbol{L} = \frac{\partial Q}{\partial t} Z \tag{11}$$

The equation mentioned in this section is very important. Because this equation is a link between the internal circuit and the external circuit. It is also noteworthy that, by calculating the surface integral $\boldsymbol{J}_D$, the displacement current $\boldsymbol{I}_D$ is obtained [142,157,163].

$$\boldsymbol{I}_D = \int \boldsymbol{J}_D \cdot d\boldsymbol{s} = \int \frac{\partial \boldsymbol{D}}{\partial t} \cdot d\boldsymbol{s} = \frac{\partial}{\partial t} \int (\nabla \cdot \boldsymbol{D}) dr = \frac{\partial}{\partial t} \int \rho dr = \frac{\partial Q}{\partial t} \tag{12}$$

The following results are based on the fact that Q is a free charge of the electrode [142]:

- The displacement current is the internal driving force in TENGs. While conducting current, the received current is on the load.
- Ideally, the conduction current is equal to the displacement current.
- The conduction current and the displacement current form a complete loop in the TENG electrodes (where they are connected). Moreover, using formal physical and equivalent electrical circuit models, the TENG outputs are fully predictable [157].

In general, there are four main modes for TENG, each of them with unique features and benefits, see Figure 3, i.e., freestanding triboelectric layer mode, single electrode mode, lateral sliding mode and contact separation mode. The general basis of the TENG function, in all modes, is the transfer of electrostatic charges to the electrodes. All TENG modes, except single electrode mode, use two electrodes. When a displacement is applied to one of the TENG layers, the state is out of electrostatic mode and a potential difference occurs. The current from the external charge is driven by such a potential difference to balance the electrostatic state. It should be mentioned that moving in the contrary direction of the TENG layer will induce an inverse potential difference between the electrodes. Hence, by having a reciprocating motion, an AC output can be received from TENG [164–166].

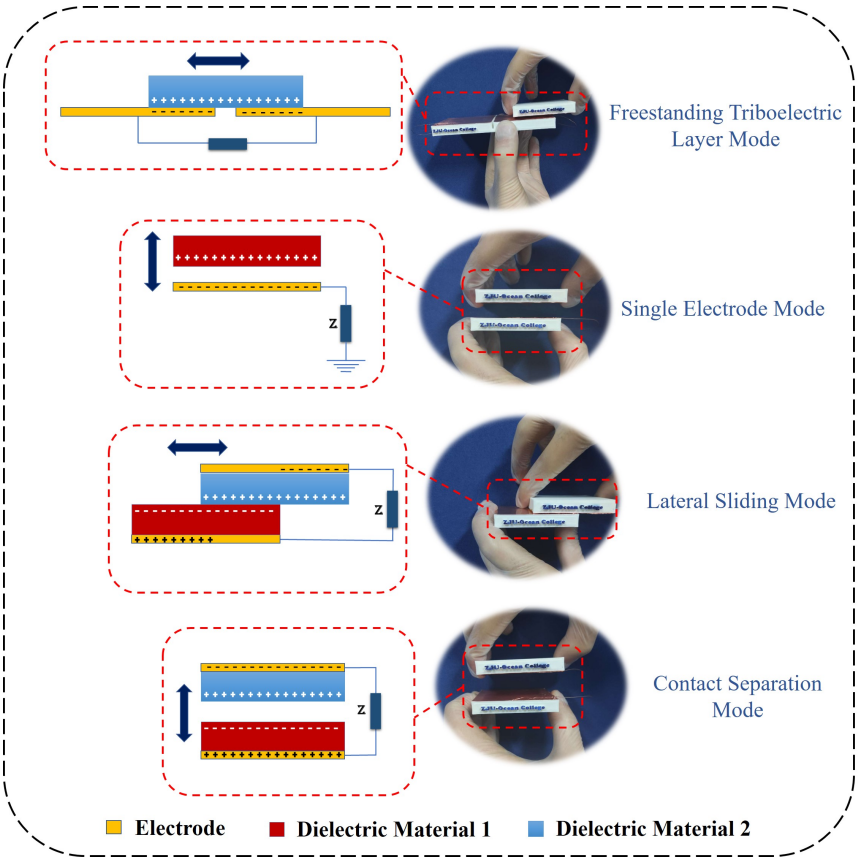

Figure 3. Four principal modes of TENGs: Contact separation, lateral sliding, single electrode and freestanding triboelectric layer (Note: Photo by authors).

The contact separation mode consists of two electrodes, which are located behind the TENG-layers. In this case, a potential difference occurs when the contact and separation processes takes place. The output voltage can be measured using a voltmeter by connecting it to one electrode and the other end to the other electrode. Then, periodically contact and disconnect operation and the output voltage can observed [167–169].

The lateral sliding mode consists of two electrodes, which, like the contact separation mode and freestanding triboelectric layer mode, are located behind the TENG layers. The TENG-layers' relative slip creates the lateral sliding mode, the state removed from the

electrostatic state and a potential difference. In this case, using a simple voltmeter, the resulting voltage can be measured. It is enough to connect one end of the voltmeter to one electrode and the other end of the voltmeter to another electrode. With the reciprocating slip of the TENG layer, the voltage created by the potential difference can be seen [169]. One of the most significant drawbacks of the lateral sliding mode and contact separation mode is that both electrodes must have an output wire, limiting their applications. A solution to solve this problem is to provide a single electrode mode. In this case, only one electrode is used. When the TENG layer comes in contact with the electrode, the condition goes out of the electrostatic state and the potential difference causes an electric current [168–173]. In this case, known as freestanding triboelectric layer mode, the TENG layer is self-moving without connecting to the electrode and the two electrodes are spaced apart. When the TENG layer slips from the first electrode to the second electrode, it causes a potential difference. In this case, to display the output voltage, it is enough to use a simple voltmeter [174]. Connect one end of the voltmeter to one electrode and the other end of the voltmeter to the other electrode. Then, by moving the TENG layer back and forth from one electrode to another, the voltage can be display by the voltmeter [175].

Figure 4a demonstrates the trends of publications about the energy harvesting system base on the TENG. Once the TENG technology was discovered around 2012, many researchers turned to work in this field and the number of published articles has increased significantly. This can be considered a turning point in the field of mechanical energy harvesting [176]. Figure 4b shows various applications of TENGs. After a decade of working on nanogenerators, researchers have demonstrated many applications and potentials in this field. TENGs are not only useful in the production of hydropower and wind energy; they can also be used in medical, civil engineering (such as structural health monitoring (SHM) systems [177] and self-power sensors as an energy source for some structures like a bridge) and other fields to protect the environment and reduce fossil fuel production [176] (Note: Various images are adopted from [176,177]).

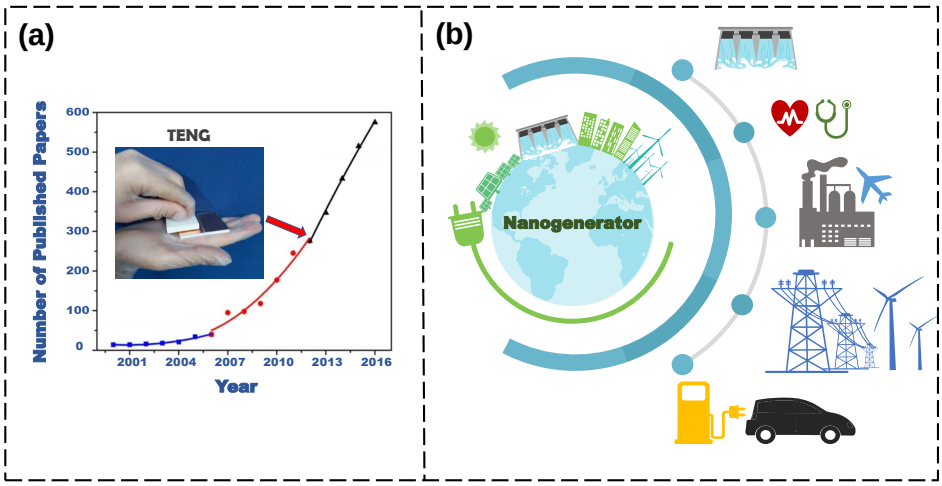

Figure 4. Trends of TENG-related publications and the applications: (**a**) Trends of publications on the energy harvesting concept and TENG's impact [176]. (**b**) Various applications of TENG.(Note: Various images are adopted from [176,177] and photo by authors)

2.4. Spherical Triboelectric Nanogenerator Networks

Figure 5a illustrates blue energy, including solar panels, wind turbines and TENGs. This design provides a concept to combine all three sources of energy as networks. However, the main problem is transporting the voltage and power to a port to be used in the city. On the other hand, this structure must be fixed to islands or underwater mountains to prevent its movement and protect marine life [104]. Figure 5b illustrates the split ball–shell structured TENG principle with silicone rubber balls and outer shells. By rotating, silicone

rubber balls from one layer to another can transfer electrons and generate a high and efficient voltage from ocean waves. This design is a network that can be located on the surface of the water [178]. Figure 5e also supports this concept with different materials and different connections [19].

Figure 5c shows spherical TENG networks with different operations. In this design, when the ocean waves come from any direction, the pendulum can rotate freely and transfer electrons between layers to harvest energy [179–181]. Figure 5d illustrates another concept of spherical TENG networks with a different structure. The principle of this design is based on the movement of polyacrylate balls between several layers of spherical TENG [182]. The main advantage of the all-spherical design is that it can work in any ocean wave direction.

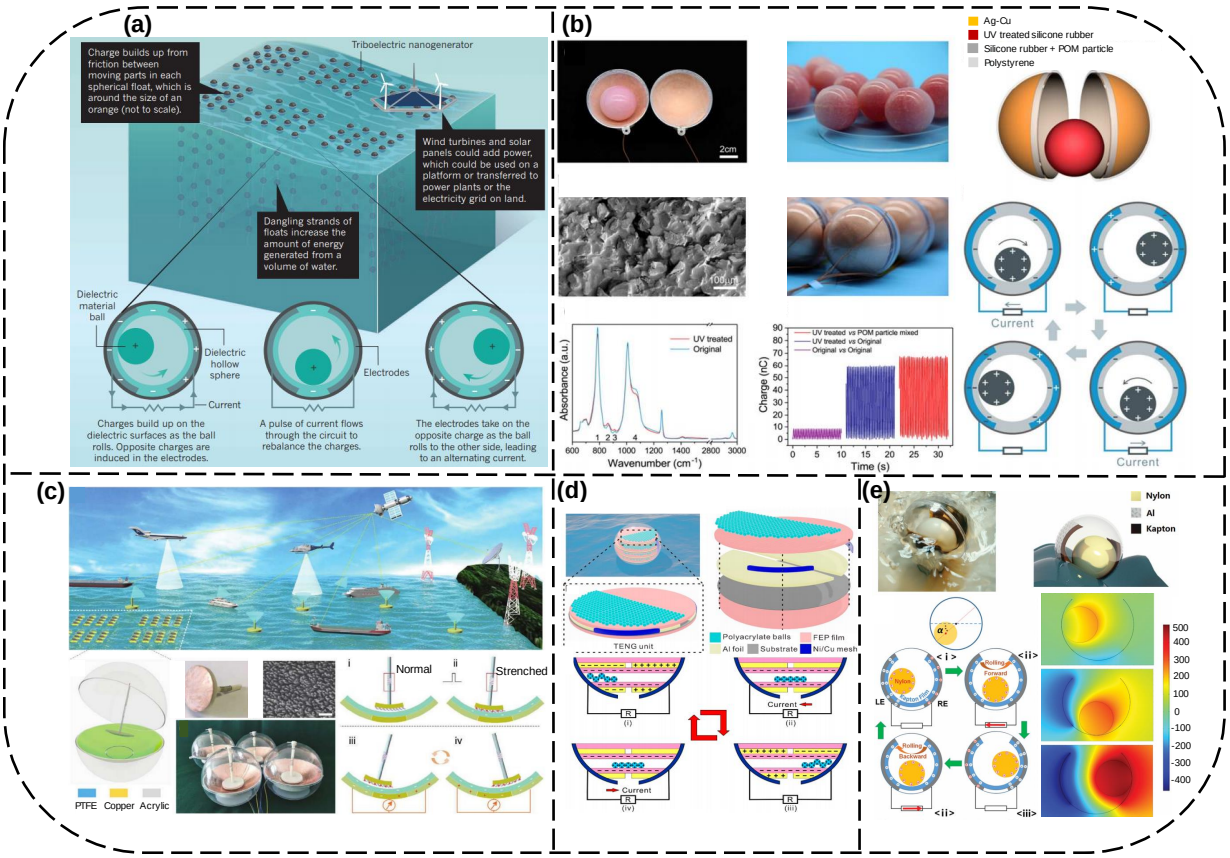

Figure 5. Spherical TENG Networks: (**a**) Harvest renewable energy from the ocean using floating nets of nanogenerators [104]. (**b**) Design and working principle of the split ball–shell structured TENG with silicone rubber balls and outer shells [178]. (**c**) Principle of the ES-TENG networks for collecting energy from ocean waves [179]. (**d**) Theory of the spherical TENG with dense point contacts [182]. (**e**) Freestanding-triboelectric-layer nanogenerator's design and working principles (RF-TENG) with a rolling nylon ball enclosed [19]. Note: Various images are adopted from [19,104,178,179,182].

2.5. Spring-Assisted Triboelectric Nanogenerator

TENG without help from other components such as spring and magnet are more productive for harvesting energy. Nevertheless, ocean waves have a lower frequency, which may cause some difficulties in generating a very restricted electrical energy. Some gadget TENGs use springs to collect unstable dynamic energy that perform poorly concerning high-frequency oscillations and enable energy transformation efficiency. Figure 6a presents a conceptual framework of tandem TENG with a cascade impact structure (CIT-TENG) for generating energy from different layers of TENG (TENG-1, TENG-2, TENG-3 and TENG-4) with various frequencies for each TENG layer. The tribo-layer used in this design is PTEF and the electrode is aluminum. In this design, having a small vibration, all TENG

layers move with different frequencies and generate energy based on the contact mode of TENGs [183].

Figure 6b presents a TENG built on a suspended 3D spiral structure that is assisted by mass and spring. In this method, the frequency can be increased by changing the mass and spring values to develop output voltage from ocean waves. Contact separation mode is also used in this structure. A triboelectric layer is Kapton and the electrode is aluminum [23]. Figure 6c illustrates the working principle of a spring-assisted TENG based on the vertical contact separation mode. In this method, the spring is used to increase the high-frequency oscillations and generate more dynamic energy. In this structure, the triboelectric layer is PTFE and the electrode is copper [184–186].

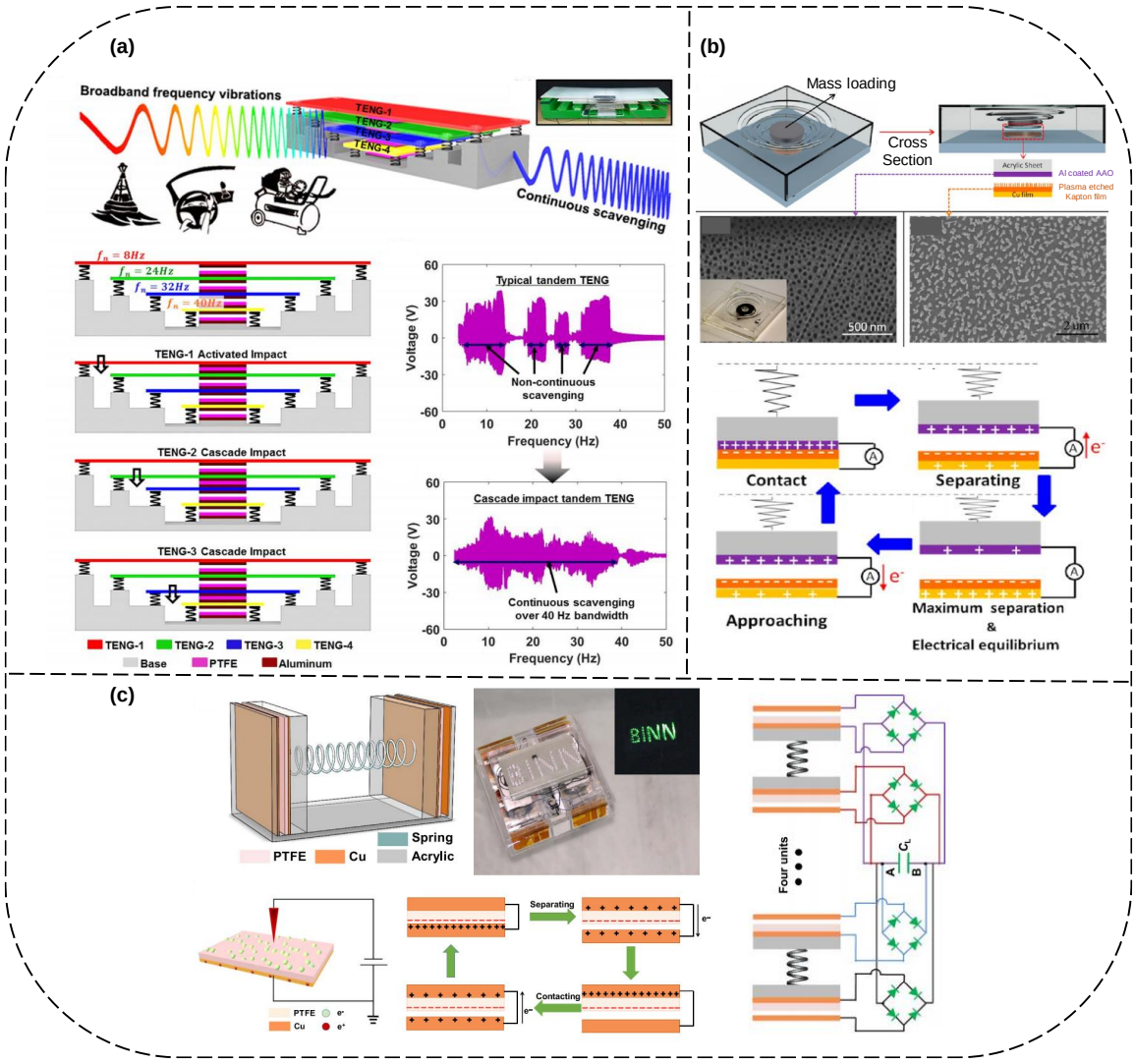

Figure 6. Spring-assisted TENGs: (**a**) Conceptual and cross-section schematic of the CIT-TENG design with output voltage [183]. (**b**) Principle of TENG built on a suspended 3D spiral structure [23]. (**c**) Principal and fabrication of spring-assisted TENG device with process for generating negative charges on the surface of PTFE [184]. Note: Various images are adopted from [23,183,184].

2.6. Liquid–Solid Interfacing Triboelectric Nanogenerator

TENGs based on liquid–solid contact have numerous benefits such as increasing output voltage from ocean wave energy, improving contact area between the FEP film and water and having a simple structure. Figure 7a shows the conceptual framework of a liquid–solid electrification-enabled generator (LSEG). In this design, the structure

will be located in front of the wave and when the wave is contacted, water will come up and water will cross from one layer to another to transfer the electron [27,187–191]. Figure 7b presents the structure of a novel wave sensor based on a liquid–solid interfacing triboelectric nanogenerator (WS-TENG), which is useful for structural health monitoring of marine equipment. The triboelectric layer used in this design is PTEF and the electrode is copper. The principle of this method is based on the water which can come up and the water will cross from one layer to another for electron exchange [192]. As shown in Figure 7c, this structure can harvest energy by the network of the liquid–solid-contact buoy TENGs from ocean waves. The innovation of this design includes two external and internal layers of TENG, which can generate energy from the shaking and rotating movement of waves [26]. Figure 7d illustrates the mechanism of droplet-based TENGs for wave energy harvesting (DB-TENG) for marine vehicles. The principle of this design is also based on the water. The triboelectric layer used in this structure is FEP and the electrode is copper [193,194].

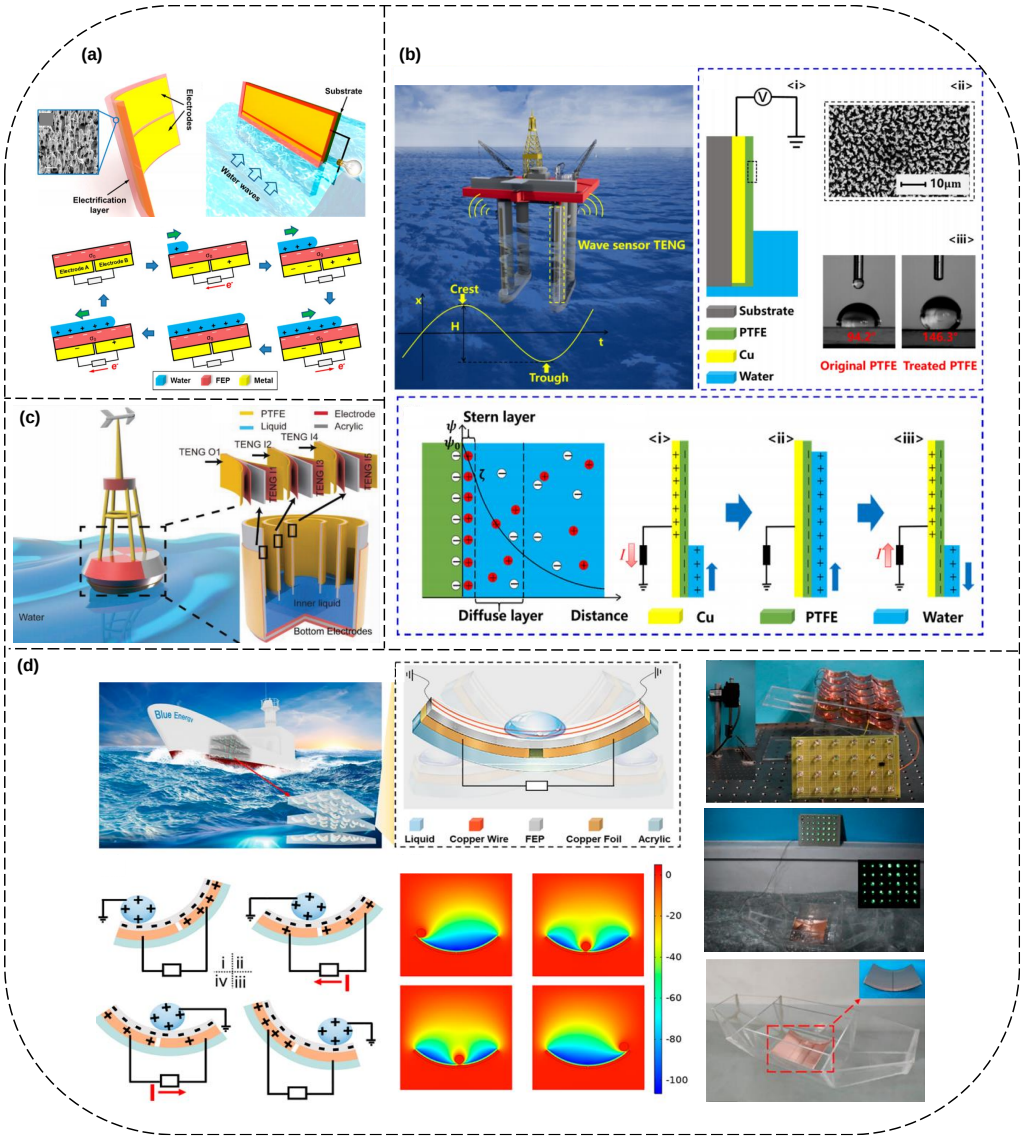

Figure 7. Liquid–solid interfacing TENGs: (**a**) Structural design of liquid–solid electrification enabled generator (LSEG) [27]. (**b**) Principal of a novel wave sensor based on liquid–solid interfacing triboelectric nanogenerator (WS-TENG) useful for monitoring waves around marine equipment [192]. (**c**) Structural design of the blue energy harvested by the network of the liquid–solid-contact buoy TENGs [26]. (**d**) Working mechanism of droplet-based TENG for wave energy harvesting (DB-TENG) [193]. Note: Various images are adopted from [26,27,192,193].

3. Hybridization of TENG with Other Energy Harvester Systems

So far, the concept of TENG, its applications, mechanism and different modes have been discussed. However, it is always challenging to improve the efficiency of TENGs by combining them with other energy-generating systems. The resulting hybrid system will benefit from advantages of both systems. In this section, the TENG is hybridized with solar cells, electromagnetic systems and some others.

3.1. Hybridized Piezoelectric and TENG

Figure 8a describes a high output piezo/triboelectric hybrid generator. This hybrid generator merges triboelectric output voltage and a high piezoelectric output current, which generates a peak voltage of ∼370 V, a current density of ∼12 μA cm^{-2} and the average power density ∼4.44 mW cm^{-2}. The amount of power strongly turned on 600 LED bulbs by applying a mechanical force of 0.2 N and it is able to charge a 10 μF capacitor to 10 V during 25 s [195].

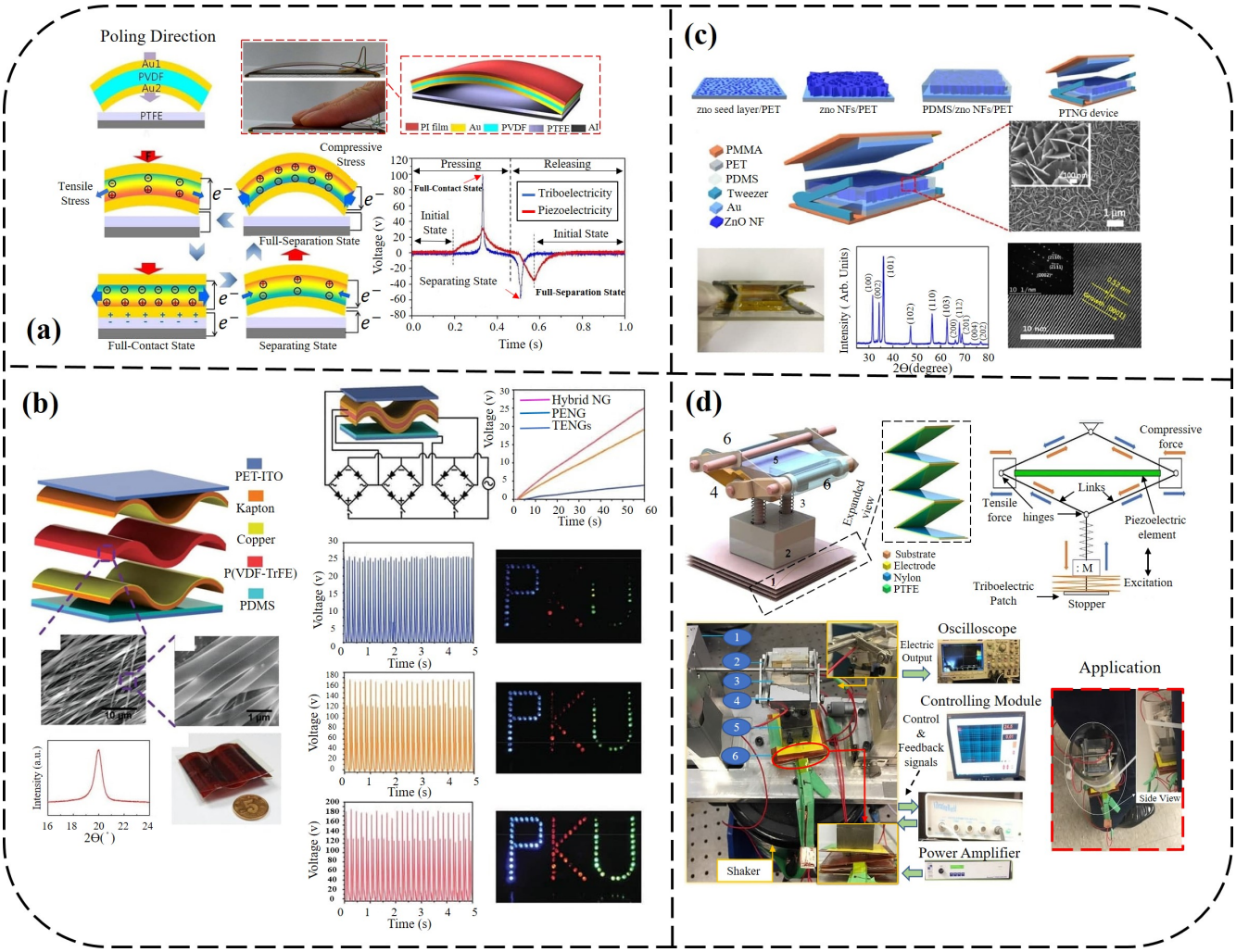

Figure 8. Different structures and their application of a piezoelectric and TENG: (**a**) Schematic of a working mechanism of the hybrid generator in a press and release cycle [195]. (**b**) Structure design of the wave-shaped hybrid piezoelectric and TENG based on P(VDF-TrFE) nanofibers [196]. (**c**) Schematic illustration and characterizations of the PTNG devices based on ZnO nanoflakes/polydimethylsiloxane composite films [197]. (**d**) Structural configuration of the generator for low-frequency and broad-bandwidth energy harvesting [198]. Note: Various images are adopted from [195–198].

In Figure 8b, a wave-shaped hybrid piezoelectric and TENG is illustrated founded on P(VDF-TrFE) nanofibers. In this technique, a piezoelectric P(VDF-TrFE) nanofiber is sandwiched between two wave-shaped Kapton films to form a three-layer pattern. This

structure produces piezoelectric triboelectric outputs concurrently in one press and release cycle. Within well-organized experimental validation and situational analysis, the three-layer fabrication can produce noticeable output performance for both parts. Meanwhile, triggered with 4 Hz external force, the piezoelectric part produces a peak output and current of 96 V and 3.8 μA, which is ∼2 times higher than its first output. While the execution of triboelectric parts increases 8 V and 16 V with the support of piezoelectric potential [196].

Figure 8c presents ultrahigh output piezoelectric and triboelectric association nanogenerators based on ZnO nanoflakes/polydimethylsiloxane composite films. There is a hybrid nanogenerator (NG) utilizing both piezoelectric and triboelectric effects influenced from ZnO nanoflakes (NFs)/polydimethylsiloxane (PDMS) composite films by a facile, cost-effective fabrication design. This hybrid NG showed high piezoelectric output current owing to the improved surface piezoelectricity of the ZnO NFs, including high triboelectric output voltage owing to the notable triboelectrification of Au-PDMS contact, generating a voltage of ∼470 V, a current density of ∼60 μA. cm^{-2} and an average power density of ∼28.2 mW. cm^{-2}. The hybrid NGs with a space of 3 × 3 cm^2 immediately turned on 180 green light-emitting diodes within cyclic control compression [197].

In Figure 8d, a hybrid piezoelectric-triboelectric generator is depicted for low-frequency and broad-bandwidth energy harvesting. The generator is created using a piezoelectric energy harvester (PEH) patch, a TENG patch, a spring-mass method and an amplitude limiter. The spring-mass method takes energy from applied excitation and utilizes forces to the piezoelectric component and the triboelectric films. The novel amplitude limiter is deliberately organized inside the system, obtaining the effect of favorable frequency up-conversion increasing the voltage responses considerably. Moreover, the limiter creates hardening nonlinearity and dynamic bifurcation triggering super harmonic resonance due to resonation concerning the generator at a cycle of approximately 3 Hz. The implemented PEH adopts the extreme compressive performance mode and employs a truss mechanism to amplify the impact forces effectively. The open-circuit voltages following excitation of 1.0 g at resonance are 58.4 V and 60 V from PEH and TENG, respectively. The hybridized generator produces the highest power of 19.6 mW from two sources by matched impedances. The working bandwidths of the PEH and the TENG are increased to 5.39 Hz and 7.25 Hz, respectively. Meanwhile, the applications to charge capacitors, the high saturation voltage and the approximately short charging time validate the effectiveness of the power management technique. Besides, the generator is useful to efficiently scavenge energy from human body actions and charge a capacitor of 4.7 μF to 7.6 V in approximately 50 s. It shows a high potential of functional usages in wearable mechanisms [198].

3.2. Hybridized Solar Cells and TENG

Figure 9a describes integrating a TENG with a silicon solar cell by an electrode for harvesting energy from sunlight and raindrops. A heterojunction silicon (Si) solar cell is combined with a TENG using a mutual electrode of a poly (3.4-ethylene dioxythiophene):poly (styrene sulfonate) (PEDOT:PSS) film. The solar cell, printed PEDOT:PSS is applied to decrease light reflection, which begins to improve short-circuit current density. A single-electrode-setup water-drop TENG on the solar cell is made with merging imprinted polydimethylsiloxane (PDMS) as a triboelectric material merged with a PEDOT:PSS layer as an electrode. The expanding contact section among the imprinted PDMS and water drops considerably increases the voltage output of the TENG with a peak short-circuit current of ∼33.0 nA and a peak open-circuit voltage of ∼2.14 V, sequentially [67].

Figure 9b illustrates biomimetic anti-reflective TENGs for concurrent harvesting of solar and raindrop energies. A moth's eye mimicking TENG (MM-TENG) can perform the role of equivalent energy harvester to a standard solar cell due to its higher specular transmittance (maximum 91% for visible light). At the first time, strongly examine the visible effect of the MM-TENG on a solar cell by considering solar-weighted transmittance (SWT). The 0.01% developed SWT in the MM-TENG enhances the fill part and power

transformation efficiency of the solar cell by 0.5% and 0.17%, respectively, compared with a traditional protective glass plate that constantly utilized a solar panel. Moreover, in addition to such prominent high transmittance, the self-cleaning property of the MM-TENG enables the long-term production of the solar panel. Besides, this design summarizes a unique electric circuit for effective control in a hybrid energy harvester through intermittently transferring the preserved electrical energy output of the MM-TENG [121].

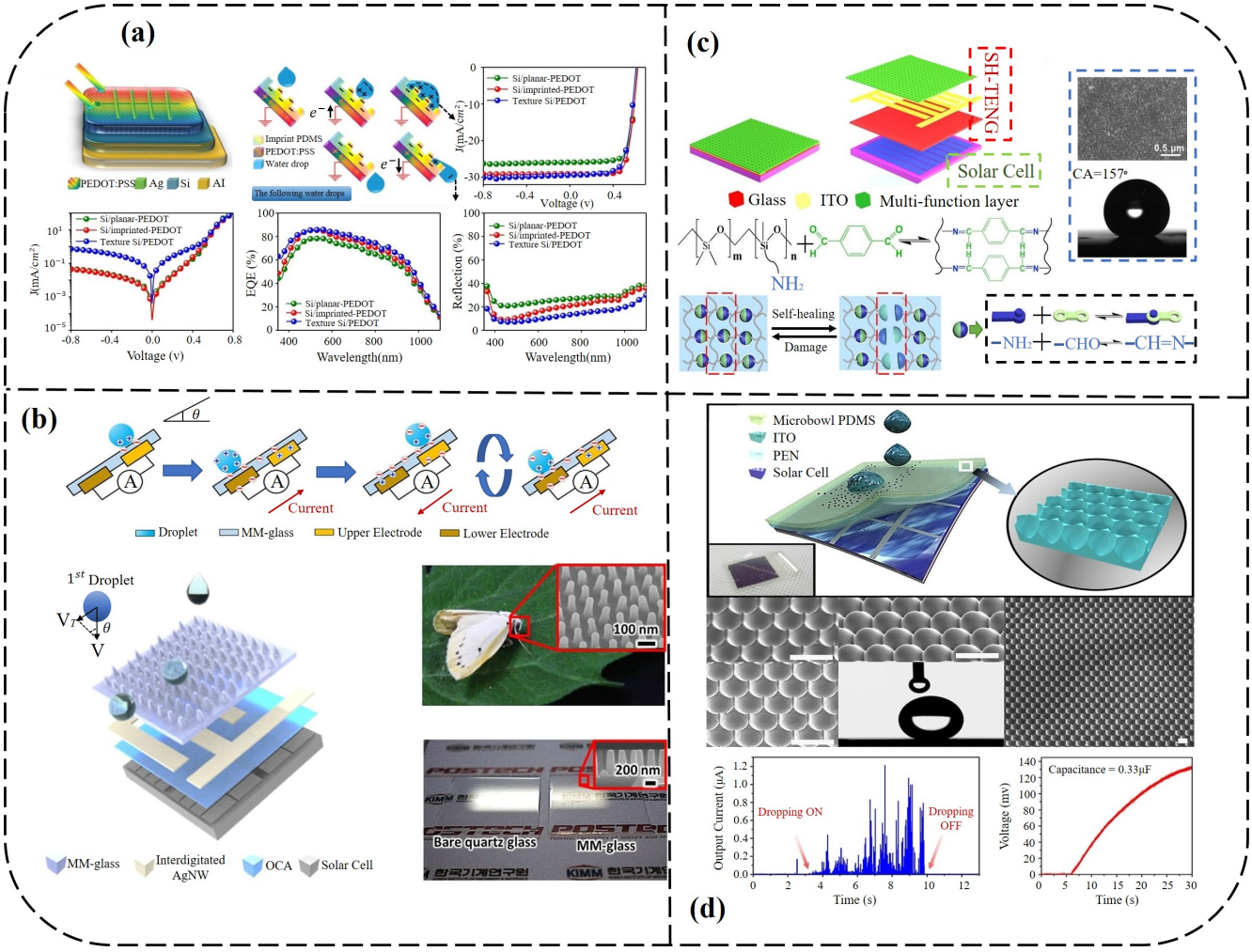

Figure 9. Various structures of integrating TENG with solar cells: (**a**) Schematic of a working mechanism of integrating a silicon solar cell with a TENG via a mutual electrode for harvesting energy from sunlight and raindrops [67]. (**b**) Structure design of the biomimetic anti-reflective TENG for concurrent harvesting of solar and raindrop energies [121]. (**c**) Schematic diagram of the hybrid energy system with the SH-TENG and solar cell [199]. (**d**) Structural configuration of the self-cleaning hybrid energy harvester to generate power from raindrop and sunlight [105]. Note: Various images are adopted from [67,105,121,199].

Figure 9c shows a hybrid energy system based on solar cells and a self-healing/self-cleaning TENG. This self-healable and transparent TENG presents an outstanding output execution on a rainy day with a peak short-circuit current of 0.8 μA and a peak open-circuit voltage of 6 V, separately. At the same time, it can work very strongly beside the solar cell on sunny days. Moreover, the self-healing TENG with elastic composition can function as a protection film for the solar cell, where the of the solar cell's risk of breakinfg can be significantly overcome [199].

Figure 9d shows a self-cleaning hybrid energy harvester to generate power from raindrops and sunlight. The transparent TENG made with superhydrophobic PDMS and ITO/PEN substrate. The amount of voltage current was 7 V and 128 nA, separately.

The highest output power is 0.27 μW. Additionally, output components of water TENG are studied with several solutions such as natural rainwater and flowing water to investigate the sensible potential of water TENG in harvesting actual raindrop energy [105].

3.3. Hybridized TENG with Electromagnetic

Figure 10a demonstrates a self-powered and self-functional tracking system-based triboelectric-electromagnetic hybridized blue energy harvesting module. A sophisticated designed rotating gyro structure, including a triboelectric-electromagnetic working principle, strongly established a battery-less tracking method. The unique gyro rolling mode solution of the TENG features its sensitivity, multiple directions and robustness. Eventually, the triboelectric-electromagnetic hybridized module was completely confirmed autonomously within the Huanghai Sea project [200].

Figure 10b shows a hybridized triboelectric-electromagnetic water wave energy harvester (WWEH) based on a magnetic sphere. A freely rolling magnetic sphere senses the water movement to drive the friction object sliding on a solid surface for TENG back and forth. Simultaneously, two coils convert the motion of the magnetic sphere into electricity based on the electromagnetic induction effect. Harvesting the blue energy from any place, the electrodes of the TENG are determined as the Tai Chi form, the effectiveness of which is analyzed and described. According to experimental results, the two friction films and two coils are given in parallel and series connection. A paper-based super-capacitor of ∼1 mF is fabricated to save the generated energy. The WWEH is located on a buoy to examine in Lake Lanier. The super-capacitor can be charged to 1.84 V and the electric energy storage approximately 1.64 mJ during 162 s [201].

Figure 10c presents the complementary electromagnetic-triboelectric active sensor (ETAS) for detecting multiple mechanical triggerings. This work displays a combined ETAS for simultaneous detection of various mechanical triggering signals. The high-grade combination of a contact-separation mode TENG and an electromagnetic generator (EMG) recognizes the complements of their incomparable benefits. The logical consideration of EMG and TENG analysis are presented to explain the relation of output and the external mechanical signals. Corresponding to the experimental outcomes, the output voltage of the TENG part recognizes the magnitude of the external triggering force with a sensibility of around 2.01 VN^{-1}, while the output current of the EMG part is more suitable to showing that the triggering speed and the sensation is approximately 4.3 mA s/m. Furthermore, both the TENG and EMG parts display high stability after 20,000 cycles of force loading–unloading [202].

Figure 10d demonstrates an ultra-low-friction triboelectric-electromagnetic hybrid nanogenerator for generating energy as a self-powered sensor. A freestanding mode TENG and a rotating EMG are combined to recognize unique merits. The principal is based on contact between soft and flexible triboelectric elements in the TENG outputs with low friction force. The impressions of the model and the dimensions of the dielectric material on the performance of the TENG are regularly considered in hypotheses concerning experiments. According to the results, voltage output is improved by the rotation velocity, which is very different from a standard rotary TENG and is due to the contact area's increase. The optimized TENG has a maximal load voltage of 65 V and maximal load power per unit mass of 438.9 mW/kg under a velocity rotation of 1000 rpm. The EMG has a maximal load voltage of 7 V and a maximal load power density of 181 mW/kg. This illustrates that the hybrid NG can power various sensors such as humidity and temperature by converting wind energy within electric energy during wind speeds of 5.7 m/s. In contrast, it can be utilized as a self-powered wind velocity sensor to recognize wind rates as low as 3.5 m/s [203].

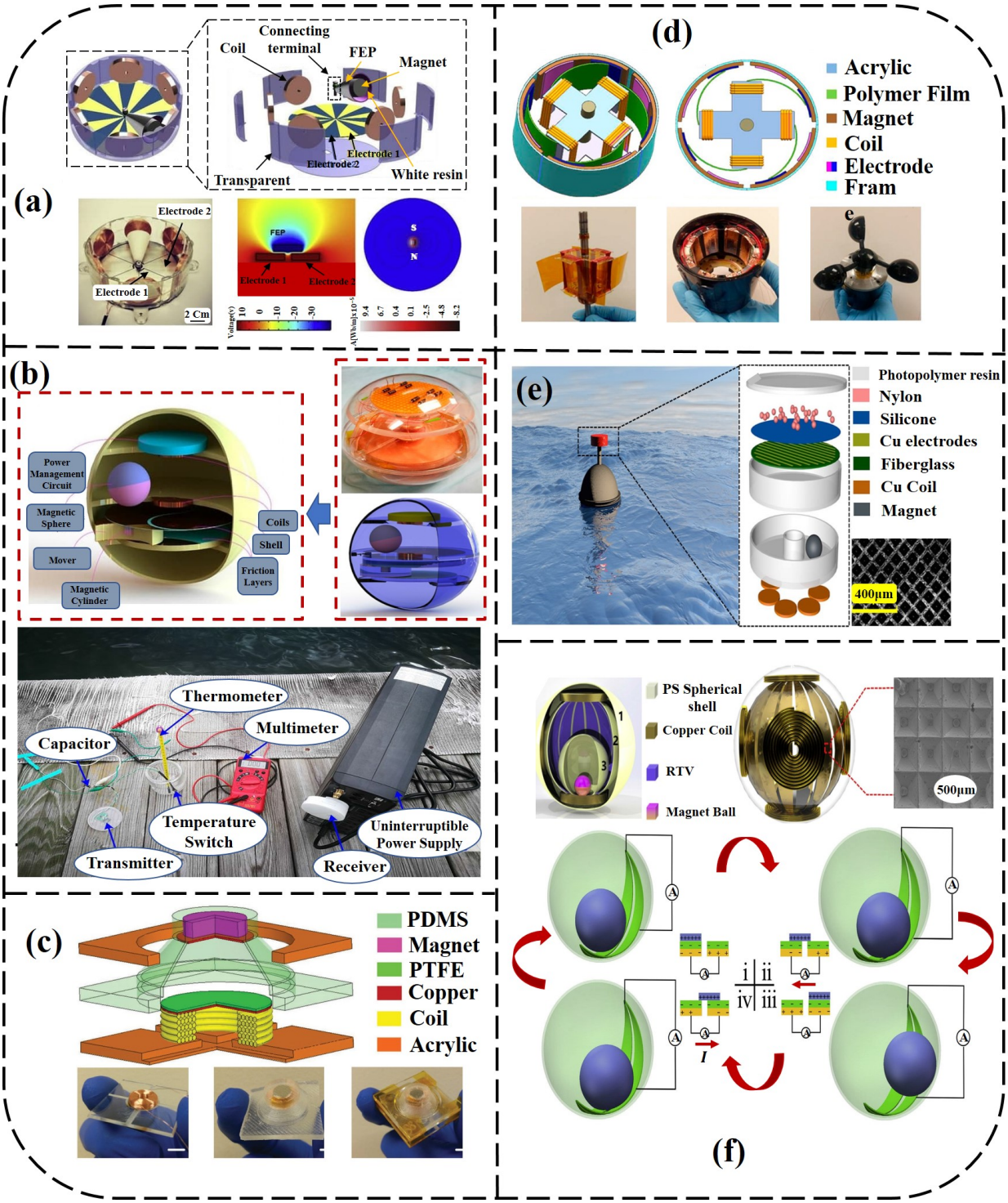

Figure 10. Various structures of hybridized electromagnetic-triboelectric nanogenerators: (**a**) Structure and working principle of a self-powered and self-functional tracking system based on a triboelectric-electromagnetic hybridized sort [200]. (**b**) Structure and illustration of the working principle of the hybridized triboelectric-electromagnetic water wave energy harvester (WWEH) [201]. (**c**) Structure design of the hybridized EMG-TENG active sensor [202]. (**d**) Working principle of an ultra-low-friction triboelectric-electromagnetic hybrid nanogenerator for rotation energy harvesting and self-powered wind speed sensor [203]. (**e**) Structural diagram of the pendulum hybrid generator used in a hydrophone-based system with the scanning electron microscopy (SEM) image of the silicone film [204]. (**f**) Schematic diagrams of the FSHG internal structure and SEM image of surface microstructure with the charge generation process in TENG modules [205]. Note: Various images are adopted from [200–205].

Figure 10e illustrates a pendulum hybrid generator for water wave energy harvesting and hydrophone-based wireless sensing. The aimed pendulum fabrication can harvest irregular water wave energy from random directions sensitively. Combining a freely rolling mode TENG and a magnetic sphere-based EMG produces complementary benefits and harvests wave energy in a wide frequency range. The hybrid generator is shown to drive 177 LEDs and power electronic equipment. At a wave driving rate of 1.4 Hz, the output power of the EMG and TENG is 6.7 mW and 8.01 μW, sequentially. A capacitor in this design can be charged to 26 V by the hybridized generator in 200 s by 1.8 Hz [204].

Figure 10f shows a 3D full-space triboelectric-electromagnetic hybrid nanogenerator toward high-efficient mechanical energy harvesting in a vibration method. The output voltage of the field test demonstrated the performance of TENG and EMGs, which can be influenced by the direction of external vibration and excitation frequency. The result of output voltage of TENG and EMGs develops as the excitation frequency rises. The outcome explains that the maximum output power of TENG is 18 mW at an external loading resistance of 200 MΩ and the maximum output power of EMG is 640 mW at an external loading resistance of 1000 Ω. The FSHG displays a fast-charging capacity for capacitor and the capability to power hundreds of LEDs. After saving energy within the capacitor, the DC signal can power a humidity/temperature sensor [205].

3.4. Hybridized TENG with Magnetic Intensity

Figure 11a demonstrates a self-powered multi-functional motion sensor enabled by a magnetic-regulated TENG. Typically, a self-powered multi-functional movement sensor (MFMS) is aimed in this design to detect the motion parameters such as area, velocity and acceleration of linear and rotary movements concurrently. The MFMS is made of a TENG module, a magnetic regulation module and an acrylic shell. The mode of TENG used in this structure is free standing with a polytetrafluorethylene (PTFE) plate and six copper electrodes. The working mechanism of the MFMS design is based on the sliding of the MD on the PTFE plate for electron exchange between layers. The precisely designed six copper electrodes can detect eight directions of action with the acceleration and determine the rotational velocity and direction.

Furthermore, the magnetic regulation module is utilized here by fixing a magnetic cylinder (MC) in the shell, right below the center of the PTFE plate. Because of the magnetic attraction utilized by the MC in this design, the MD will automatically return to the center to prepare for the next discovery round, making the proposed sensor much more suitable for practice [206].

Figure 11b illustrates wind energy and blue energy harvesting according to the magnetic-assisted noncontact TENG. An innovative approach to wind and blue energy harvesting based on a magnetic-assisted noncontact TENG has been described. With the compound of the magnetic responsive composite with the TENG design, the wind and water forces could be transformed toward the contact-separation movement between Al/Ni electrode and PDMS film. The influence of the related parameters (contact-separation frequency, wind speed and humidity) on the performances of the fabricated TENG has been regularly examined. The results explain the strong potential of magnetic-assisted noncontact TENG for wind and blue energy harvesting purposes [207].

Figure 11c shows a floating oscillator-embedded triboelectric generator (FO-TEG) for versatile mechanical energy harvesting. The FO-TEG is appropriate for impulse excitation and sinusoidal vibration, which are in the natural ecosystem. For the impulse excitation, the created current sustains and moderately decays by the residual oscillation of the floating oscillator. Resonance oscillation maximizes the output energy for sinusoidal vibration. The acting frequency range can be optimized via a high degree of freedom to satisfy different application requirements. Furthermore, the highest resistance to ambient humidity is empirically illustrated, which stems from the inherently packaged fabrication of FO-TEG. The prototype design presents a peak-to-peak open-circuit voltage of 157 V and an instantaneous short-circuit current of 4.6 μA, within sub-10 Hz of operating frequency [208].

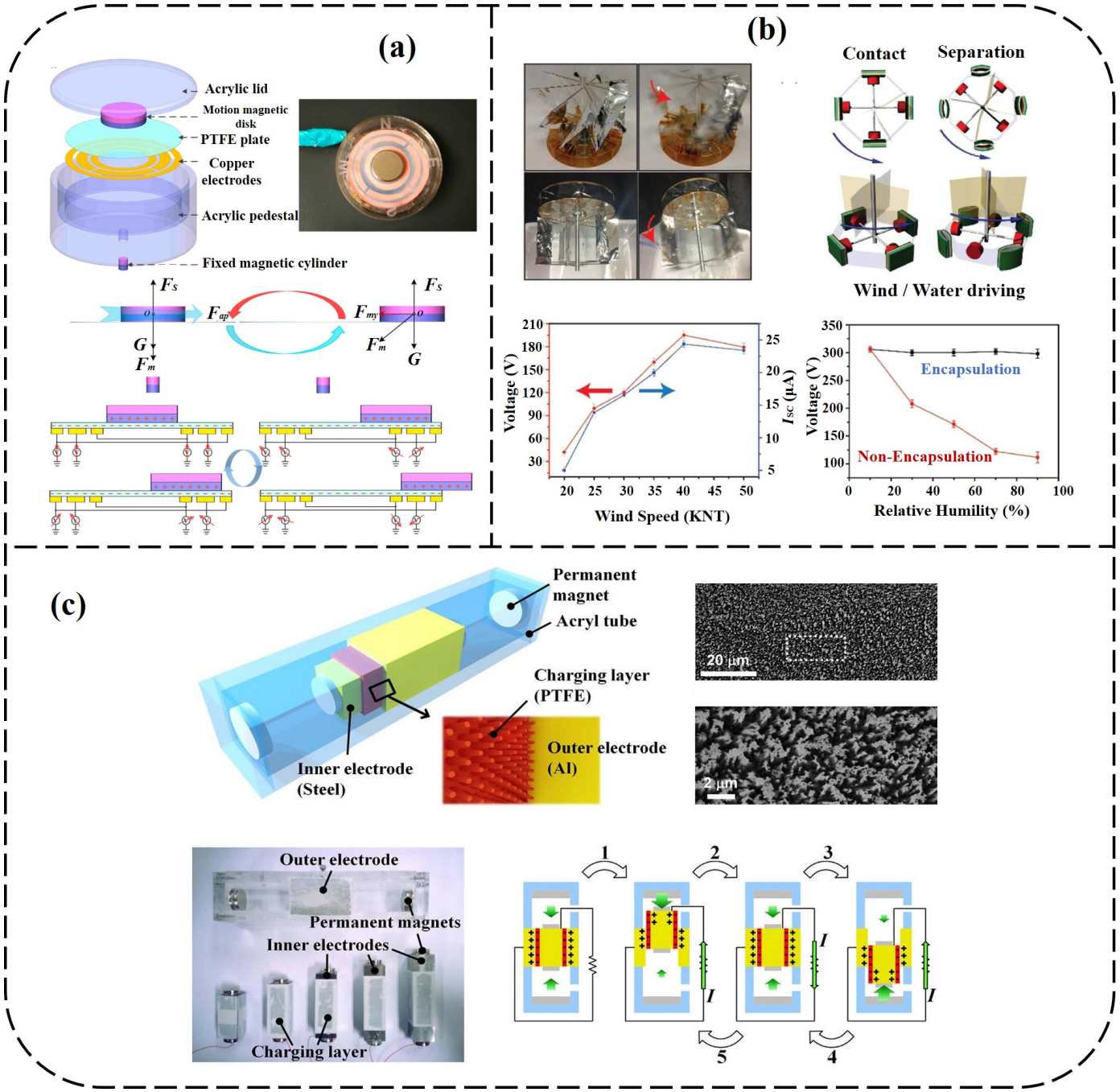

Figure 11. Various structures combining TENG with magnetic intensity: (**a**) Structure and illustration of the working principle of a self-powered multi-functional motion sensor (MFMS) [206]. (**b**) Demonstration and schematic illustration of magnetic-assisted noncontact TENG for harvesting energy from wind and water flow (four devices arranged with perpendicular angle) [207]. (**c**) Schematic illustration of the FO-TEG structure. The FO-TEG contains a tube part with a mobile oscillator part floating inside, suspended by magnetic repulsive forces. Vertical nanowire-like structures are formed on the sidewalls of the PTFE charging layer [208]. Note: Various images are adopted from [206–208].

Figure 12a demonstrates a magnetic switch structured TENG for continuous and regular wind energy harvesting. A magnetic switch structured triboelectric nanogenerator (MS-TENG) is developed, consisting of transmission gears, energy modulation modules and a creation unit. Meanwhile, wind falls intermittently on the wind scoop; the energy collected and released through the energy modulation do not depend on wind velocity. However, the magnetic force of the magnets allows the wind energy to be changed into continuous and normal electric energy. The experimental outcomes show that the MS-

TENG can succeed as a power supply, generating output characteristics of 410 V, 18 μA, 155 nC and peak power of 4.82 mW, satisfactory to power 500 LEDs in series [209].

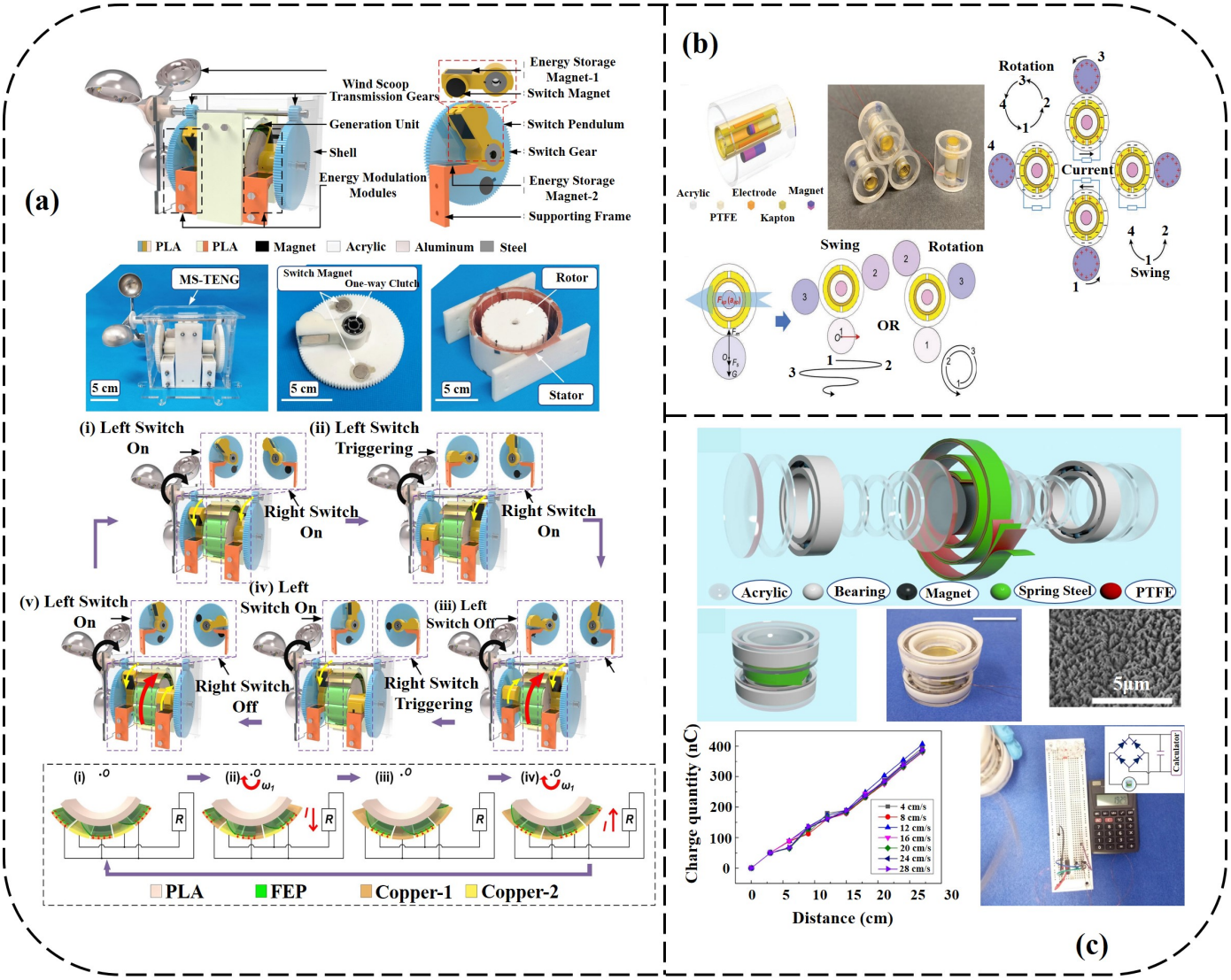

Figure 12. Various structures of hybridized TENG using magnetic intensity. (**a**) The magnetic switch structured triboelectric nanogenerator (MS-TENG) [209]. (**b**) Structural design and working principle of the multifunctional sensor based on translational-rotary triboelectric nanogenerator [210]. (**c**) Schematic illustrating the structure of assembled and digital photo of MR-TENG [211]. Note: Various images are adopted from [209–211].

Figure 12b explains a multi-functional sensor according to a translational rotary TENG. A cylindrical self-powered multi-functional sensor (MS) with a translational-rotary magnetic mechanism aims to recognize acceleration, force and rotational parameters. The MS can convert a translational movement into a swing motion or a multi-cycle rotational movement of a low damping magnetic cylinder around a friction layer, therefore driving the TENG to produce voltage output. To augment the TENG's output performance, an electrode material with a small work function, low resistance and suitable surface topography is the best choice. Based on the fabrication characteristic of the translational rotary magnetic mechanism, the MS can simply respond to a low striking and can measure the rotational parameters without the need for coaxial installation. According to the MS, some applications are installed [210].

Figure 12c shows a novel TENG relying on magnetically induced retractable spring steel tapes (MR-TENG) for efficient energy harvesting of large amplitude periodic motion.

An ingenious design utilizes a new material. The tape-like fundamental design ensures that the contact/separate direction of the friction layers is straight concerning the force direction, breaking the amplitude limitation of prior nanogenerators with vertical contact/separate movement. Conjunction of flexible spring steel tapes makes the structure of design enable portability, therefore widening its application. The outcomes present that the maximum short-circuit current, open-circuit voltage and instantaneous power are 21 μA, 342 V and 1.8 mW, sequentially [211].

3.5. Comparison of TENG Structures

Figure 13 illustrates the advantages and disadvantages of various design strategies for TENGs, including spherical TENG networks, spring-assisted TENGs, liquid–solid interfacing TENGs, hybridized piezoelectrics and TENGs, hybridized solar cells and TENGs, hybridized TENGs with electromagneticm and finally hybridized TENGs with magnetic intensity.

Figure 13. Advantages and disadvantages of different TENG structures.

4. Applications, Challenges and Future Trends of TENGs

The quest to find new (and also renewable) energy resources has always been a key point in modern history. Traditional sources like coal and oil are associated with a lot of pollution, as well as climate change. Therefore, the majority of recent efforts have been concentrated on clean energy resources. In the last decade, one of the most significant human discoveries in this field is the triboelectric nanogenerator. As discussed in Figure 4b, TENG has a broad domain of applications in human life, from medical sciences to engineering and technology.

Maybe two of the most interesting applications for TENG can be found in the civil engineering field. The first one is associated with the SHM of large bridges. For such infrastructure, not all parts are easily accessible by the technicians to install the sensors for damage detection purposes. These sensors require a continuous source of energy to be able to detect the vibrations, analyze them and transmit data to the center. Since the installation

and maintenance of the batteries for these sensors are very difficult, an alternative can be to use a TENG as an energy source. On the other hand, TENGs can be used even in a larger scale to supply the required energy for smart cities.

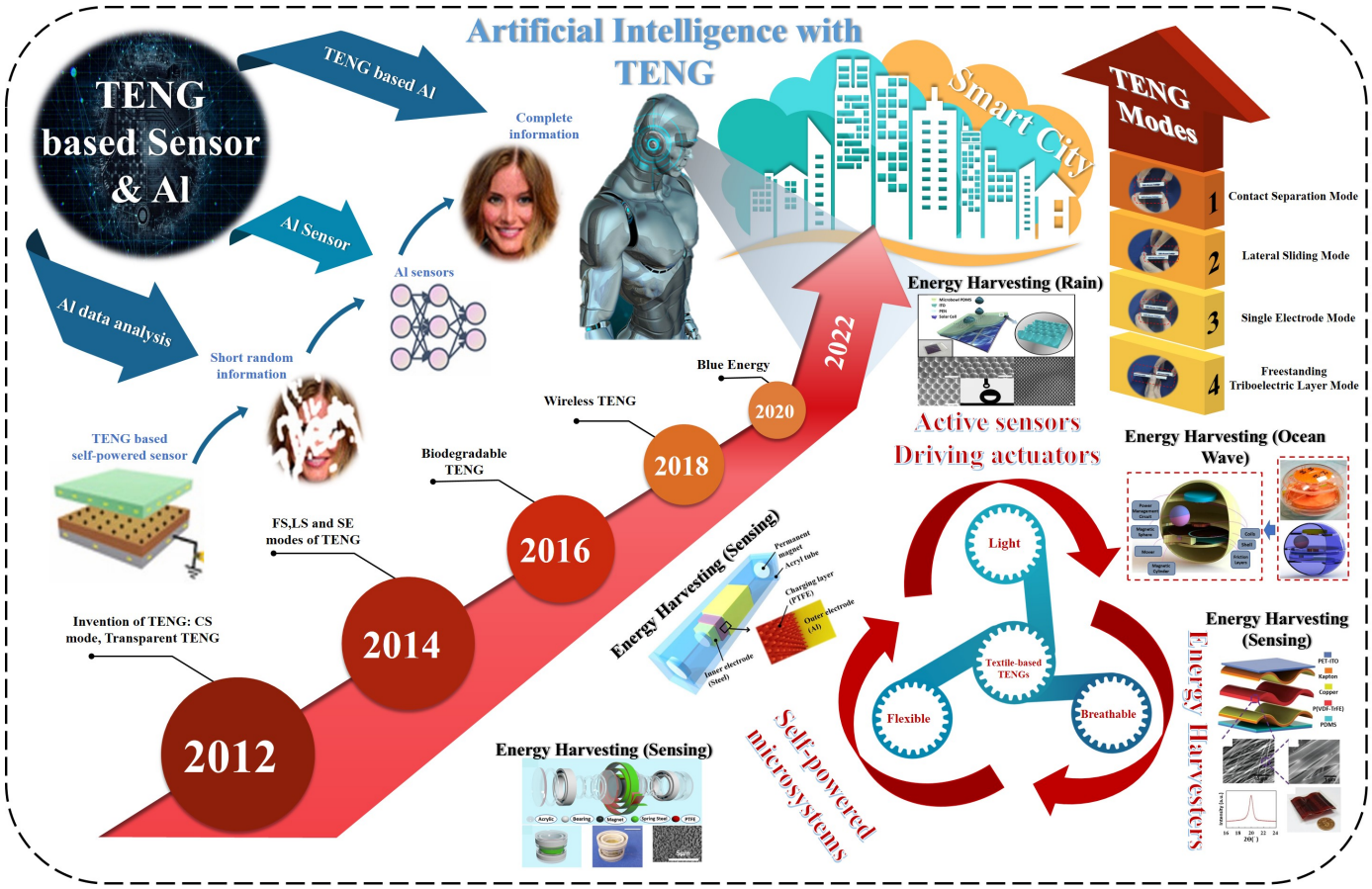

Figure 14. A summary of recent progress in development of TENGs from 2012 to 2022 including the future trends and their connection with AI.

Figure 14 shows the challenges and future trends related to TENGs. In January 2012, professor Zhong Lin Wang introduced the principle of another type of TENG, which can also harvest ambient mechanical energy by combining contact-electrification and the electrostatic phenomenon. The TENG concept has been expanded to biodegradable TENGs, wireless TENGs and blue energy and more recently in smart cities. TENGs also have a bright future in robotics and self-powered sensing technologies when they are combined with artificial intelligence (AI). TENGs have been proposed in ubiquitous computation, which presents the potential of applying them to increase an entire sensor network.

Table 3 presents the performance output comparison of various TENG devices to collect ocean wave energy such as spherical TENG networks, spring-assisted TENG, liquid–solid interfacing TENG, hybridized piezoelectrics and TENGs, hybridized solar cell sand TENGs, electromagnetic hybridized TENGs and hybridized TENGs with magnetic intensity. Most of the electrodes used in TENG are Al and Cu and also most of the triboelectric layers are PTFE.

Table 3. Summary of various hybridized TENG techniques to harvest ocean energy.

Structure	Year	Authors	Applied Tribo-Layer	Electrode Type	Max-Open-Circuit Voltage (V)	Max-Short-Circuit Current (μA)	Current Density	Surface Power Density	Power Density and Power	Load Resistance (Ω)
Spherical TENG Networks	2018	Xu et al. [178]	Polystyrene	Ag-Cu	1780	1.8	-	-	4.47 W/m^3	1 GΩ
	2021	Lin et al. [179]	PTFE	Cu	76	4.4	-	-	28 μW	100 MΩ
	2022	Yuan et al. [182]	FEP	Ni/Cu-Al	2103	15.5	-	-	20.57 W/m^3	300 MΩ
	2015	Wang [19]	Nylon 6/6 and Kapton	Al	903	1	-	-	10 mW	10 GΩ
Spring-assisted TENG	2019	Bhatia et al. [183]	PTFE	Al	14	0.75	-	-	-	40 GΩ
	2013	Hu et al. [23]	Kapton	Al/Cu	150	27	20 mA/m^2	2.76 W/m^2	-	6 MΩ
	2016	Jiang et al. [184]	PTFE	Cu	755.8	65	-	-	-	-
Liquid–solid interfacing TENG	2014	Zhu et al. [27]	FEP	Cu	3	-	-	-	0.12 μW	150 MΩ
	2019	Xu et al. [192]	PTFE	Cu	1.98	-	-	-	-	-
	2018	Li et al. [26]	PTFE/FEP/FET/PDMS	Cu/Al	600	9	-	-	-	
	2021	Wei et al. [193]	FEP	Cu	237	746 nA	-	-	23.3 μW	500 MΩ
Hybridized PENG and TENG	2015	Jung et al. [195]	PTFE	Al/Au	370	12	-	4.4 mW/cm^2	-	-
	2018	He et al. [197]	PDMS/NFs	Au	470	60	-	28.2 mW/cm^2	-	-
	2017	Chen et al. [196]	Kapton/PDMS	Cu	361.27	10.85	-	-	441μW	100 MΩ
	2018	Li et al. [198]	PTFE	Nylon	60	-	-	-	5.7 mW	1 MΩ
Hybridized TENG with solar cells	2018	Liu et al. [67]	PDMS/PEDOT:PSS	Al/Ag	2.14	33 nA	-	-	-	-
	2015	Jeon et al. [105]	PDMS	ITO/PEN	7	128 nA	-	27 μW	25 MΩ	
	2019	Yoo et al. [121]	MM-glass	AgNW	18.4	24.4	-	-	-	-
	2021	Yang et al. [199]	Silicone	ITO	6	0.8	-	-	-	-
Hybridized TENG with EMG	2020	Gao et al. [200]	FEP	PCB	23.76	-	-	-	-	-
	2019	Wu et al. [201]	PTFE	Cu	172.95	3.5	-	-	-	-
	2018	Wang et al. [203]	Polymer	Cu	65	-	-	-	438.9 mW/kg	-
	2020	Hao et al. [204]	Silicone	Cu/Nylon	72	1.7	-	-	8.01 μW	1 MΩ
	2018	Wang et al. [202]	PTFE/PDMS	Cu	13.1	0.25	-	-	-	-
	2020	He et al. [205]	Silicone	Cu	88	-	-	-	18 μW	200 MΩ
Hybridized TENG with magnetic intensity	2018	Wu et al. [206]	PTFE	Cu	∼ 2	-	-	-	-	-
	2015	Seol et al. [208]	PTFE	Al	157	4.6	-	-	-	-
	2016	Huang et al. [207]	PDMS	Al/Ni	206	30	-	-	3 mW	10 MΩ
	2021	Liu et al. [209]	FEP	Cu	410	18	-	-	4.82 mW	50 MΩ
	2019	Wu et al. [210]	Kapton/PTFE	Ag/Au/Cu/ITO	1.75	70 nA	-	-	-	-
	2017	Liu et al. [211]	PTFE	Spring steel	342	21	-	-	1.8 mW	2 MΩ

5. Summary

This paper reviews and summarizes the concept of triboelectric nanogenerators (TENGs) for energy harvesting purposes from ocean waves. This review covers the TENGs from the fabrication of the design to the working principle, the recent improvements and various applications for ocean waves energy. The TENG technology that aims at numerous environmental energies is extensively utilized in the energy storage unit, which can be useful for self-power sensors. Furthermore, conjunction nanogenerators of a TENG and various types of power sources have been discussed for ocean as an innovative technology approach. Through this study, the emerging TENG technology has displayed a high potential in several fields from medical science to engineering.

It is expected that, with the current growth in TENG technology, as well as its hybridization with other energy sources, more efficient applications could be identified in the near future. This study provided a condensed (yet comprehensive) review of the current improvements in TENGs and the relevant technologies. First, we present the characteristics of ocean wave energy, followed by the underpinning principles of TENGs. Next, the function of hybridization of TENGs with another type of energy harvester and the various structural designs of TENGs as energy harvesters have been discussed. In addition, future improvements in TENG technology including a self-powered sort combined with sensors and actuators have been studied. Finally, the expansion of TENGs has been summarized and future challenges and opportunities have been briefly explained. Low motion frequency is the most important characteristic of ocean energy, so it can be considered an energy harvester application based on the TENG. Figure 15 shows a summary of the cloud words used in this review paper highlighting the most frequent words.

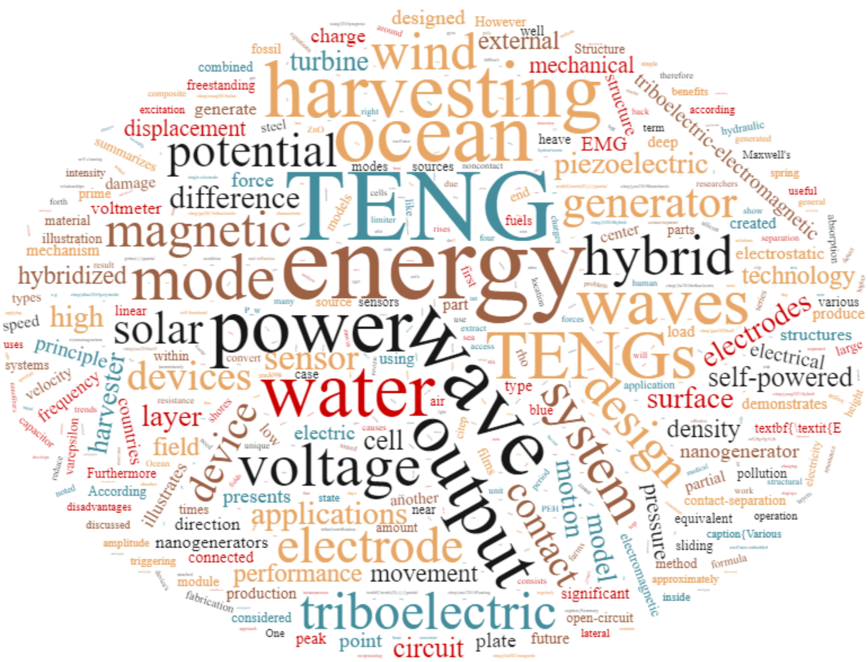

Figure 15. Word cloud summarizing the most frequent statements in this paper.

Author Contributions: Conceptualization, A.M.N.; investigation, A.M.N., K.-J.I.E., A.A., M.A.H.-A.; writing—original draft preparation, A.M.N.; writing—review and editing, A.M.N., K.-J.I.E., A.A., M.A.H.-A.; visualization, A.M.N., A.A., M.A.H.-A.; Supervision, M.A.H.-A.; project administration, M.A.H.-A. All authors have read and agreed to the published version of the manuscript.

Funding: This research received no external funding.

Conflicts of Interest: The authors declare no conflict of interest.

References

1. Atzori, L.; Iera, A.; Morabito, G. The internet of things: A survey. *Comput. Netw.* **2010**, *54*, 2787–2805. [CrossRef]
2. Santoro, G.; Vrontis, D.; Thrassou, A.; Dezi, L. The Internet of Things: Building a knowledge management system for open innovation and knowledge management capacity. *Technol. Forecast. Soc. Chang.* **2018**, *136*, 347–354. [CrossRef]
3. Wang, X.; Song, J.; Liu, J.; Wang, Z.L. Direct-current nanogenerator driven by ultrasonic waves. *Science* **2007**, *316*, 102–105. [CrossRef]
4. Wang, S.; Xie, Y.; Niu, S.; Lin, L.; Wang, Z.L. Freestanding triboelectric-layer-based nanogenerators for harvesting energy from a moving object or human motion in contact and non-contact modes. *Adv. Mater.* **2014**, *26*, 2818–2824. [CrossRef] [PubMed]
5. Wang, Z.L.; Jiang, T.; Xu, L. Toward the blue energy dream by triboelectric nanogenerator networks. *Nano Energy* **2017**, *39*, 9–23. [CrossRef]
6. Fan, F.R.; Tian, Z.Q.; Wang, Z.L. Flexible triboelectric generator. *Nano Energy* **2012**, *1*, 328–334. [CrossRef]
7. Wang, Z.L. Triboelectric nanogenerators as new energy technology for self-powered systems and as active mechanical and chemical sensors. *ACS Nano* **2013**, *7*, 9533–9557. [CrossRef]
8. Wang, Z.L.; Chen, J.; Lin, L. Progress in triboelectric nanogenerators as a new energy technology and self-powered sensors. *Energy Environ. Sci.* **2015**, *8*, 2250–2282. [CrossRef]
9. Qin, H.; Cheng, G.; Zi, Y.; Gu, G.; Zhang, B.; Shang, W.; Yang, F.; Yang, J.; Du, Z.; Wang, Z.L. High energy storage efficiency triboelectric nanogenerators with unidirectional switches and passive power management circuits. *Adv. Funct. Mater.* **2018**, *28*, 1805216. [CrossRef]
10. Kammen, D.M.; Sunter, D.A. City-integrated renewable energy for urban sustainability. *Science* **2016**, *352*, 922–928. [CrossRef]
11. Liu, J.; Cui, N.; Gu, L.; Chen, X.; Bai, S.; Zheng, Y.; Hu, C.; Qin, Y. A three-dimensional integrated nanogenerator for effectively harvesting sound energy from the environment. *Nanoscale* **2016**, *8*, 4938–4944. [CrossRef] [PubMed]
12. Javadi, M.; Heidari, A.; Darbari, S. Realization of enhanced sound-driven CNT-based triboelectric nanogenerator, utilizing sonic array configuration. *Curr. Appl. Phys.* **2018**, *18*, 361–368. [CrossRef]
13. Zhao, C.; Zhang, Q.; Zhang, W.; Du, X.; Zhang, Y.; Gong, S.; Ren, K.; Sun, Q.; Wang, Z.L. Hybrid piezo/triboelectric nanogenerator for highly efficient and stable rotation energy harvesting. *Nano Energy* **2019**, *57*, 440–449. [CrossRef]
14. Feng, A.S.; Narins, P.M. Ultrasonic communication in concave-eared torrent frogs (*Amolops tormotus*). *J. Comp. Physiol. A* **2008**, *194*, 159–167. [CrossRef]
15. Xi, Y.; Wang, J.; Zi, Y.; Li, X.; Han, C.; Cao, X.; Hu, C.; Wang, Z. High efficient harvesting of underwater ultrasonic wave energy by triboelectric nanogenerator. *Nano Energy* **2017**, *38*, 101–108. [CrossRef]
16. Painuly, J.P. Barriers to renewable energy penetration; a framework for analysis. *Renew. Energy* **2001**, *24*, 73–89. [CrossRef]
17. Reddy, S.; Painuly, J.P. Diffusion of renewable energy technologies—Barriers and stakeholders' perspectives. *Renew. Energy* **2004**, *29*, 1431–1447. [CrossRef]
18. Wang, Z.L. Catch wave power in floating nets. *Nat. News* **2017**, *542*, 159. [CrossRef] [PubMed]
19. Wang, Z.L. Triboelectric nanogenerators as new energy technology and self-powered sensors–Principles, problems and perspectives. *Faraday Discuss.* **2015**, *176*, 447–458. [CrossRef] [PubMed]
20. Gandomi, A.H.; Alavi, A.H.; Asghari, A.; Niroomand, H.; Matin Nazar, A. An innovative approach for modeling of hysteretic energy demand in steel moment resisting frames. *Neural Comput. Appl.* **2014**, *24*, 1285–1291. [CrossRef]
21. Jiao, P.; Egbe, K.J.I.; Xie, Y.; Matin Nazar, A.; Alavi, A.H. Piezoelectric sensing techniques in structural health monitoring: A state-of-the-art review. *Sensors* **2020**, *20*, 3730. [CrossRef] [PubMed]
22. Matin Nazar, A.; Jiao, P.; Zhang, Q.; Egbe, K.J.I.; Alavi, A.H. A New Structural Health Monitoring Approach Based on Smartphone Measurements of Magnetic Field Intensity. *IEEE Instrum. Meas. Mag.* **2021**, *24*, 49–58. [CrossRef]
23. Hu, Y.; Yang, J.; Jing, Q.; Niu, S.; Wu, W.; Wang, Z.L. Triboelectric nanogenerator built on suspended 3D spiral structure as vibration and positioning sensor and wave energy harvester. *ACS Nano* **2013**, *7*, 10424–10432. [CrossRef]
24. Lin, Z.H.; Cheng, G.; Lin, L.; Lee, S.; Wang, Z.L. Water–solid surface contact electrification and its use for harvesting liquid-wave energy. *Angew. Chem. Int. Ed.* **2013**, *52*, 12545–12549. [CrossRef] [PubMed]
25. Zhao, X.J.; Kuang, S.Y.; Wang, Z.L.; Zhu, G. Highly adaptive solid–liquid interfacing triboelectric nanogenerator for harvesting diverse water wave energy. *ACS Nano* **2018**, *12*, 4280–4285. [CrossRef]
26. Li, X.; Tao, J.; Wang, X.; Zhu, J.; Pan, C.; Wang, Z.L. Networks of high performance triboelectric nanogenerators based on liquid–solid interface contact electrification for harvesting low-frequency blue energy. *Adv. Energy Mater.* **2018**, *8*, 1800705. [CrossRef]
27. Zhu, G.; Su, Y.; Bai, P.; Chen, J.; Jing, Q.; Yang, W.; Wang, Z.L. Harvesting water wave energy by asymmetric screening of electrostatic charges on a nanostructured hydrophobic thin-film surface. *ACS Nano* **2014**, *8*, 6031–6037. [CrossRef]
28. Xu, L.; Pang, Y.; Zhang, C.; Jiang, T.; Chen, X.; Luo, J.; Tang, W.; Cao, X.; Wang, Z.L. Integrated triboelectric nanogenerator array based on air-driven membrane structures for water wave energy harvesting. *Nano Energy* **2017**, *31*, 351–358. [CrossRef]
29. Lee, K.; Lee, J.W.; Kim, K.; Yoo, D.; Kim, D.S.; Hwang, W.; Song, I.; Sim, J.Y. A spherical hybrid triboelectric nanogenerator for enhanced water wave energy harvesting. *Micromachines* **2018**, *9*, 598. [CrossRef]
30. An, J.; Wang, Z.M.; Jiang, T.; Liang, X.; Wang, Z.L. Whirling-folded triboelectric nanogenerator with high average power for water wave energy harvesting. *Adv. Funct. Mater.* **2019**, *29*, 1904867. [CrossRef]

31. Feng, Y.; Ling, L.; Nie, J.; Han, K.; Chen, X.; Bian, Z.; Li, H.; Wang, Z.L. Self-powered electrostatic filter with enhanced photocatalytic degradation of formaldehyde based on built-in triboelectric nanogenerators. *ACS Nano* **2017**, *11*, 12411–12418. [CrossRef]
32. Yang, Y.; Wang, Z.L. Hybrid energy cells for simultaneously harvesting multi-types of energies. *Nano Energy* **2015**, *14*, 245–256. [CrossRef]
33. Cha, S.N.; Seo, J.S.; Kim, S.M.; Kim, H.J.; Park, Y.J.; Kim, S.W.; Kim, J.M. Sound-driven piezoelectric nanowire-based nanogenerators. *Adv. Mater.* **2010**, *22*, 4726–4730. [CrossRef]
34. Huang, L.B.; Bai, G.; Wong, M.C.; Yang, Z.; Xu, W.; Hao, J. Triboelectric Nanogenerators: Magnetic-Assisted Noncontact Triboelectric Nanogenerator Converting Mechanical Energy into Electricity and Light Emissions (Adv. Mater. 14/2016). *Adv. Mater.* **2016**, *28*, 2843. [CrossRef]
35. Cheng, G.; Lin, Z.H.; Du, Z.l.; Wang, Z.L. Simultaneously harvesting electrostatic and mechanical energies from flowing water by a hybridized triboelectric nanogenerator. *ACS Nano* **2014**, *8*, 1932–1939. [CrossRef] [PubMed]
36. Cui, N.; Gu, L.; Liu, J.; Bai, S.; Qiu, J.; Fu, J.; Kou, X.; Liu, H.; Qin, Y.; Wang, Z.L. High performance sound driven triboelectric nanogenerator for harvesting noise energy. *Nano Energy* **2015**, *15*, 321–328. [CrossRef]
37. Miles, J.W. On the generation of surface waves by shear flows. *J. Fluid Mech.* **1957**, *3*, 185–204. [CrossRef]
38. Chen, J.; Huang, Y.; Zhang, N.; Zou, H.; Liu, R.; Tao, C.; Fan, X.; Wang, Z.L. Micro-cable structured textile for simultaneously harvesting solar and mechanical energy. *Nat. Energy* **2016**, *1*, 1–8. [CrossRef]
39. Ren, Z.; Ding, Y.; Nie, J.; Wang, F.; Xu, L.; Lin, S.; Chen, X.; Wang, Z.L. Environmental energy harvesting adapting to different weather conditions and self-powered vapor sensor based on humidity-responsive triboelectric nanogenerators. *ACS Appl. Mater. Interfaces* **2019**, *11*, 6143–6153. [CrossRef]
40. Chen, J.; Yang, J.; Li, Z.; Fan, X.; Zi, Y.; Jing, Q.; Guo, H.; Wen, Z.; Pradel, K.C.; Niu, S.; et al. Networks of triboelectric nanogenerators for harvesting water wave energy: A potential approach toward blue energy. *ACS Nano* **2015**, *9*, 3324–3331. [CrossRef] [PubMed]
41. Bai, P.; Zhu, G.; Liu, Y.; Chen, J.; Jing, Q.; Yang, W.; Ma, J.; Zhang, G.; Wang, Z.L. Cylindrical rotating triboelectric nanogenerator. *ACS Nano* **2013**, *7*, 6361–6366. [CrossRef] [PubMed]
42. Ren, X.; Fan, H.; Wang, C.; Ma, J.; Li, H.; Zhang, M.; Lei, S.; Wang, W. Wind energy harvester based on coaxial rotatory freestanding triboelectric nanogenerators for self-powered water splitting. *Nano Energy* **2018**, *50*, 562–570. [CrossRef]
43. Lin, Z.; Zhang, B.; Guo, H.; Wu, Z.; Zou, H.; Yang, J.; Wang, Z.L. Super-robust and frequency-multiplied triboelectric nanogenerator for efficient harvesting water and wind energy. *Nano Energy* **2019**, *64*, 103908. [CrossRef]
44. Ahmed, A.; Hassan, I.; Hedaya, M.; El-Yazid, T.A.; Zu, J.; Wang, Z.L. Farms of triboelectric nanogenerators for harvesting wind energy: A potential approach towards green energy. *Nano Energy* **2017**, *36*, 21–29. [CrossRef]
45. Liang, Q.; Yan, X.; Gu, Y.; Zhang, K.; Liang, M.; Lu, S.; Zheng, X.; Zhang, Y. Highly transparent triboelectric nanogenerator for harvesting water-related energy reinforced by antireflection coating. *Sci. Rep.* **2015**, *5*, 1–7. [CrossRef] [PubMed]
46. Liang, Q.; Yan, X.; Liao, X.; Zhang, Y. Integrated multi-unit transparent triboelectric nanogenerator harvesting rain power for driving electronics. *Nano Energy* **2016**, *25*, 18–25. [CrossRef]
47. Lai, Y.C.; Hsiao, Y.C.; Wu, H.M.; Wang, Z.L. Waterproof fabric-based multifunctional triboelectric nanogenerator for universally harvesting energy from raindrops, wind and human motions and as self-powered sensors. *Adv. Sci.* **2019**, *6*, 1801883. [CrossRef]
48. Xu, M.; Zhao, T.; Wang, C.; Zhang, S.L.; Li, Z.; Pan, X.; Wang, Z.L. High power density tower-like triboelectric nanogenerator for harvesting arbitrary directional water wave energy. *ACS Nano* **2019**, *13*, 1932–1939. [CrossRef]
49. Yang, J.; Chen, J.; Liu, Y.; Yang, W.; Su, Y.; Wang, Z.L. Triboelectrification-based organic film nanogenerator for acoustic energy harvesting and self-powered active acoustic sensing. *ACS Nano* **2014**, *8*, 2649–2657. [CrossRef]
50. Yang, Y.; Zhang, H.; Liu, R.; Wen, X.; Hou, T.C.; Wang, Z.L. Fully enclosed triboelectric nanogenerators for applications in water and harsh environments. *Adv. Energy Mater.* **2013**, *3*, 1563–1568. [CrossRef]
51. Zhang, D.; Shi, J.; Si, Y.; Li, T. Multi-grating triboelectric nanogenerator for harvesting low-frequency ocean wave energy. *Nano Energy* **2019**, *61*, 132–140. [CrossRef]
52. Zou, Y.; Tan, P.; Shi, B.; Ouyang, H.; Jiang, D.; Liu, Z.; Li, H.; Yu, M.; Wang, C.; Qu, X.; et al. A bionic stretchable nanogenerator for underwater sensing and energy harvesting. *Nat. Commun.* **2019**, *10*, 1–10. [CrossRef] [PubMed]
53. Cheng, P.; Guo, H.; Wen, Z.; Zhang, C.; Yin, X.; Li, X.; Liu, D.; Song, W.; Sun, X.; Wang, J.; et al. Largely enhanced triboelectric nanogenerator for efficient harvesting of water wave energy by soft contacted structure. *Nano Energy* **2019**, *57*, 432–439. [CrossRef]
54. Liu, W.; Xu, L.; Bu, T.; Yang, H.; Liu, G.; Li, W.; Pang, Y.; Hu, C.; Zhang, C.; Cheng, T. Torus structured triboelectric nanogenerator array for water wave energy harvesting. *Nano Energy* **2019**, *58*, 499–507. [CrossRef]
55. Mariello, M.; Guido, F.; Mastronardi, V.; Todaro, M.; Desmaële, D.; De Vittorio, M. Nanogenerators for harvesting mechanical energy conveyed by liquids. *Nano Energy* **2019**, *57*, 141–156. [CrossRef]
56. Cao, X.; Jie, Y.; Wang, N.; Wang, Z.L. Triboelectric nanogenerators driven self-powered electrochemical processes for energy and environmental science. *Adv. Energy Mater.* **2016**, *6*, 1600665. [CrossRef]
57. Khan, U.; Kim, S.W. Triboelectric nanogenerators for blue energy harvesting. *ACS Nano* **2016**, *10*, 6429–6432. [CrossRef]
58. Gu, L.; Cui, N.; Liu, J.; Zheng, Y.; Bai, S.; Qin, Y. Packaged triboelectric nanogenerator with high endurability for severe environments. *Nanoscale* **2015**, *7*, 18049–18053. [CrossRef]

59. Fan, X.; Chen, J.; Yang, J.; Bai, P.; Li, Z.; Wang, Z.L. Ultrathin, rollable, paper-based triboelectric nanogenerator for acoustic energy harvesting and self-powered sound recording. *ACS Nano* **2015**, *9*, 4236–4243. [CrossRef] [PubMed]
60. Chen, F.; Wu, Y.; Ding, Z.; Xia, X.; Li, S.; Zheng, H.; Diao, C.; Yue, G.; Zi, Y. A novel triboelectric nanogenerator based on electrospun polyvinylidene fluoride nanofibers for effective acoustic energy harvesting and self-powered multifunctional sensing. *Nano Energy* **2019**, *56*, 241–251. [CrossRef]
61. Jing, Q.; Zhu, G.; Bai, P.; Xie, Y.; Chen, J.; Han, R.P.; Wang, Z.L. Case-encapsulated triboelectric nanogenerator for harvesting energy from reciprocating sliding motion. *ACS Nano* **2014**, *8*, 3836–3842. [CrossRef]
62. Xiao, T.X.; Jiang, T.; Zhu, J.X.; Liang, X.; Xu, L.; Shao, J.J.; Zhang, C.L.; Wang, J.; Wang, Z.L. Silicone-based triboelectric nanogenerator for water wave energy harvesting. *ACS Appl. Mater. Interfaces* **2018**, *10*, 3616–3623. [CrossRef]
63. Ahmed, A.; Saadatnia, Z.; Hassan, I.; Zi, Y.; Xi, Y.; He, X.; Zu, J.; Wang, Z.L. Self-powered wireless sensor node enabled by a duck-shaped triboelectric nanogenerator for harvesting water wave energy. *Adv. Energy Mater.* **2017**, *7*, 1601705. [CrossRef]
64. Zhang, S.L.; Xu, M.; Zhang, C.; Wang, Y.C.; Zou, H.; He, X.; Wang, Z.; Wang, Z.L. Rationally designed sea snake structure based triboelectric nanogenerators for effectively and efficiently harvesting ocean wave energy with minimized water screening effect. *Nano Energy* **2018**, *48*, 421–429. [CrossRef]
65. Zhang, L.M.; Han, C.B.; Jiang, T.; Zhou, T.; Li, X.H.; Zhang, C.; Wang, Z.L. Multilayer wavy-structured robust triboelectric nanogenerator for harvesting water wave energy. *Nano Energy* **2016**, *22*, 87–94. [CrossRef]
66. Zhu, H.R.; Tang, W.; Gao, C.Z.; Han, Y.; Li, T.; Cao, X.; Wang, Z.L. Self-powered metal surface anti-corrosion protection using energy harvested from rain drops and wind. *Nano Energy* **2015**, *14*, 193–200. [CrossRef]
67. Liu, Y.; Sun, N.; Liu, J.; Wen, Z.; Sun, X.; Lee, S.T.; Sun, B. Integrating a silicon solar cell with a triboelectric nanogenerator via a mutual electrode for harvesting energy from sunlight and raindrops. *ACS Nano* **2018**, *12*, 2893–2899. [CrossRef]
68. Yang, H.; Deng, M.; Tang, Q.; He, W.; Hu, C.; Xi, Y.; Liu, R.; Wang, Z.L. A nonencapsulative pendulum-like paper–based hybrid nanogenerator for energy harvesting. *Adv. Energy Mater.* **2019**, *9*, 1901149. [CrossRef]
69. Yang, F.; Guo, J.; Zhao, L.; Shang, W.; Gao, Y.; Zhang, S.; Gu, G.; Zhang, B.; Cui, P.; Cheng, G.; et al. Tuning oxygen vacancies and improving UV sensing of ZnO nanowire by micro-plasma powered by a triboelectric nanogenerator. *Nano Energy* **2020**, *67*, 104210. [CrossRef]
70. Qin, H.; Gu, G.; Shang, W.; Luo, H.; Zhang, W.; Cui, P.; Zhang, B.; Guo, J.; Cheng, G.; Du, Z. A universal and passive power management circuit with high efficiency for pulsed triboelectric nanogenerator. *Nano Energy* **2020**, *68*, 104372. [CrossRef]
71. Wang, Z.L. On the first principle theory of nanogenerators from Maxwell's equations. *Nano Energy* **2020**, *68*, 104272. [CrossRef]
72. Wang, Z.L. On Maxwell's displacement current for energy and sensors: The origin of nanogenerators. *Mater. Today* **2017**, *20*, 74–82. [CrossRef]
73. Zhu, G.; Pan, C.; Guo, W.; Chen, C.Y.; Zhou, Y.; Yu, R.; Wang, Z.L. Triboelectric-generator-driven pulse electrodeposition for micropatterning. *Nano Lett.* **2012**, *12*, 4960–4965. [CrossRef] [PubMed]
74. Wang, S.; Lin, L.; Wang, Z.L. Nanoscale triboelectric-effect-enabled energy conversion for sustainably powering portable electronics. *Nano Lett.* **2012**, *12*, 6339–6346. [CrossRef] [PubMed]
75. Wang, S.; Lin, L.; Xie, Y.; Jing, Q.; Niu, S.; Wang, Z.L. Sliding-triboelectric nanogenerators based on in-plane charge-separation mechanism. *Nano Lett.* **2013**, *13*, 2226–2233. [CrossRef] [PubMed]
76. Zhu, G.; Chen, J.; Liu, Y.; Bai, P.; Zhou, Y.S.; Jing, Q.; Pan, C.; Wang, Z.L. Linear-grating triboelectric generator based on sliding electrification. *Nano Lett.* **2013**, *13*, 2282–2289. [CrossRef] [PubMed]
77. Yang, Y.; Zhang, H.; Wang, Z.L. Direct-current triboelectric generator. *Adv. Funct. Mater.* **2014**, *24*, 3745–3750. [CrossRef]
78. Yang, Y.; Zhang, H.; Chen, J.; Jing, Q.; Zhou, Y.S.; Wen, X.; Wang, Z.L. Single-electrode-based sliding triboelectric nanogenerator for self-powered displacement vector sensor system. *Acs Nano* **2013**, *7*, 7342–7351. [CrossRef] [PubMed]
79. Niu, S.; Liu, Y.; Wang, S.; Lin, L.; Zhou, Y.S.; Hu, Y.; Wang, Z.L. Theoretical investigation and structural optimization of single-electrode triboelectric nanogenerators. *Adv. Funct. Mater.* **2014**, *24*, 3332–3340. [CrossRef]
80. Lin, Z.H.; Cheng, G.; Lee, S.; Pradel, K.C.; Wang, Z.L. Harvesting water drop energy by a sequential contact-electrification and electrostatic-induction process. *Adv. Mater.* **2014**, *26*, 4690–4696. [CrossRef]
81. Chen, Y.; Jie, Y.; Wang, J.; Ma, J.; Jia, X.; Dou, W.; Cao, X. Triboelectrification on natural rose petal for harvesting environmental mechanical energy. *Nano Energy* **2018**, *50*, 441–447. [CrossRef]
82. Choi, D.; Yoo, D.; Cha, K.J.; La, M.; Kim, D.S. Spontaneous occurrence of liquid–solid contact electrification in nature: Toward a robust triboelectric nanogenerator inspired by the natural lotus leaf. *Nano Energy* **2017**, *36*, 250–259. [CrossRef]
83. Qian, Y.; Nie, J.; Ma, X.; Ren, Z.; Tian, J.; Chen, J.; Shen, H.; Chen, X.; Li, Y. Octopus tentacles inspired triboelectric nanogenerators for harvesting mechanical energy from highly wetted surface. *Nano Energy* **2019**, *60*, 493–502. [CrossRef]
84. Xiong, J.; Lin, M.F.; Wang, J.; Gaw, S.L.; Parida, K.; Lee, P.S. Wearable All-Fabric-Based Triboelectric Generator for Water Energy Harvesting. *Adv. Energy Mater.* **2017**, *7*, 1701243. [CrossRef]
85. Zhao, Y.; Pang, Z.; Duan, J.; Duan, Y.; Jiao, Z.; Tang, Q. Self-powered monoelectrodes made from graphene composite films to harvest rain energy. *Energy* **2018**, *158*, 555–563. [CrossRef]
86. Zhou, Q.; Lee, K.; Kim, K.N.; Park, J.G.; Pan, J.; Bae, J.; Baik, J.M.; Kim, T. High humidity-and contamination-resistant triboelectric nanogenerator with superhydrophobic interface. *Nano Energy* **2019**, *57*, 903–910. [CrossRef]
87. Lee, J.H.; Kim, S.; Kim, T.Y.; Khan, U.; Kim, S.W. Water droplet-driven triboelectric nanogenerator with superhydrophobic surfaces. *Nano Energy* **2019**, *58*, 579–584. [CrossRef]

88. Lin, Z.H.; Cheng, G.; Wu, W.; Pradel, K.C.; Wang, Z.L. Dual-mode triboelectric nanogenerator for harvesting water energy and as a self-powered ethanol nanosensor. *ACS Nano* **2014**, *8*, 6440–6448. [CrossRef]
89. Liu, Y.; Zheng, Y.; Li, T.; Wang, D.; Zhou, F. Water-solid triboelectrification with self-repairable surfaces for water-flow energy harvesting. *Nano Energy* **2019**, *61*, 454–461. [CrossRef]
90. Yun, B.K.; Kim, H.S.; Ko, Y.J.; Murillo, G.; Jung, J.H. Interdigital electrode based triboelectric nanogenerator for effective energy harvesting from water. *Nano Energy* **2017**, *36*, 233–240.
91. Yu, A.; Chen, X.; Cui, H.; Chen, L.; Luo, J.; Tang, W.; Peng, M.; Zhang, Y.; Zhai, J.; Wang, Z.L. Self-powered random number generator based on coupled triboelectric and electrostatic induction effects at the liquid–dielectric interface. *ACS Nano* **2016**, *10*, 11434–11441. [CrossRef] [PubMed]
92. Kwak, S.S.; Lin, S.; Lee, J.H.; Ryu, H.; Kim, T.Y.; Zhong, H.; Chen, H.; Kim, S.W. Triboelectrification-induced large electric power generation from a single moving droplet on graphene/polytetrafluoroethylene. *Acs Nano* **2016**, *10*, 7297–7302. [CrossRef] [PubMed]
93. Nie, J.; Wang, Z.; Ren, Z.; Li, S.; Chen, X.; Wang, Z.L. Power generation from the interaction of a liquid droplet and a liquid membrane. *Nat. Commun.* **2019**, *10*, 1–10. [CrossRef]
94. Que, R.; Shao, Q.; Li, Q.; Shao, M.; Cai, S.; Wang, S.; Lee, S.T. Flexible nanogenerators based on graphene oxide films for acoustic energy harvesting. *Angew. Chem.* **2012**, *124*, 5514–5518. [CrossRef]
95. Kanik, M.; Say, M.G.; Daglar, B.; Yavuz, A.F.; Dolas, M.H.; El-Ashry, M.M.; Bayindir, M. A motion-and sound-activated, 3d-printed, chalcogenide-based triboelectric nanogenerator. *Adv. Mater.* **2015**, *27*, 2367–2376. [CrossRef] [PubMed]
96. Lee, J.P.; Ye, B.U.; Kim, K.N.; Lee, J.W.; Choi, W.J.; Baik, J.M. 3D printed noise-cancelling triboelectric nanogenerator. *Nano Energy* **2017**, *38*, 377–384. [CrossRef]
97. Horowitz, S.B.; Sheplak, M. Aeroacoustic applications of acoustic energy harvesting. *J. Acoust. Soc. Am.* **2013**, *134*, 4155. [CrossRef]
98. Lei, R.; Zhai, H.; Nie, J.; Zhong, W.; Bai, Y.; Liang, X.; Xu, L.; Jiang, T.; Chen, X.; Wang, Z.L. Butterfly-Inspired Triboelectric Nanogenerators with Spring-Assisted Linkage Structure for Water Wave Energy Harvesting. *Adv. Mater. Technol.* **2019**, *4*, 1800514. [CrossRef]
99. Zhong, W.; Xu, L.; Wang, H.; Li, D.; Wang, Z.L. Stacked pendulum-structured triboelectric nanogenerators for effectively harvesting low-frequency water wave energy. *Nano Energy* **2019**, *66*, 104108. [CrossRef]
100. Matin Nazar, A.; Egbe, K.J.I.; Jiao, P.; Alavi, A.H. A novel multi-mode magnetic triboelectric nanogenerator energy harvesting system. In *Behavior and Mechanics of Multifunctional Materials XV*; International Society for Optics and Photonics: San Diego, CA, USA, 2021; Volume 11589, p. 115890B.
101. Egbe, K.J.I.; Matin Nazar, A.; Jiao, P.; Alavi, A.H. Harnessing postbuckling instability of piezoelectric cylinders with corrugation for energy harvesting. In *Active and Passive Smart Structures and Integrated Systems XV*; International Society for Optics and Photonics: San Diego, CA, USA, 2021; Volume 11588, p. 115881N.
102. Horowitz, S.B.; Sheplak, M.; Cattafesta, L.; Nishida, T. A MEMS acoustic energy harvester. *J. Micromech. Microeng.* **2006**, *16*, S174. [CrossRef]
103. Varmaghani, A.; Matin Nazar, A.; Ahmadi, M.; Sharifi, A.; Jafarzadeh Ghoushchi, S.; Pourasad, Y. DMTC: Optimize Energy Consumption in Dynamic Wireless Sensor Network Based on Fog Computing and Fuzzy Multiple Attribute Decision-Making. *Wirel. Commun. Mob. Comput.* **2021**, *2021*, 9953416. [CrossRef]
104. Wang, Z.L. New wave power. *Nature* **2017**, *542*, 159–160. [CrossRef] [PubMed]
105. Jeon, S.B.; Kim, D.; Yoon, G.W.; Yoon, J.B.; Choi, Y.K. Self-cleaning hybrid energy harvester to generate power from raindrop and sunlight. *Nano Energy* **2015**, *12*, 636–645. [CrossRef]
106. Hu, Y.; Wang, Z.L. Recent progress in piezoelectric nanogenerators as a sustainable power source in self-powered systems and active sensors. *Nano Energy* **2015**, *14*, 3–14. [CrossRef]
107. Guillou, N.; Thiébot, J.; Chapalain, G. Turbines' effects on water renewal within a marine tidal stream energy site. *Energy* **2019**, *189*, 116113. [CrossRef]
108. Falnes, J. A review of wave-energy extraction. *Mar. Struct.* **2007**, *20*, 185–201. [CrossRef]
109. Su, Y.; Wen, X.; Zhu, G.; Yang, J.; Chen, J.; Bai, P.; Wu, Z.; Jiang, Y.; Wang, Z.L. Hybrid triboelectric nanogenerator for harvesting water wave energy and as a self-powered distress signal emitter. *Nano Energy* **2014**, *9*, 186–195. [CrossRef]
110. Giassi, M.; Göteman, M. Layout design of wave energy parks by a genetic algorithm. *Ocean Eng.* **2018**, *154*, 252–261. [CrossRef]
111. Wu, C.; Wang, A.C.; Ding, W.; Guo, H.; Wang, Z.L. Triboelectric nanogenerator: A foundation of the energy for the new era. *Adv. Energy Mater.* **2019**, *9*, 1802906. [CrossRef]
112. Jiang, D.; Liu, G.; Li, W.; Bu, T.; Wang, Y.; Zhang, Z.; Pang, Y.; Xu, S.; Yang, H.; Zhang, C. A leaf-shaped triboelectric nanogenerator for multiple ambient mechanical energy harvesting. *IEEE Trans. Power Electron.* **2019**, *35*, 25–32. [CrossRef]
113. Yang, Y.; Zhang, H.; Lin, Z.H.; Liu, Y.; Chen, J.; Lin, Z.; Zhou, Y.S.; Wong, C.P.; Wang, Z.L. A hybrid energy cell for self-powered water splitting. *Energy Environ. Sci.* **2013**, *6*, 2429–2434. [CrossRef]
114. Yang, X.; Zhu, G.; Wang, S.; Zhang, R.; Lin, L.; Wu, W.; Wang, Z.L. A self-powered electrochromic device driven by a nanogenerator. *Energy Environ. Sci.* **2012**, *5*, 9462–9466. [CrossRef]
115. Algie, C.; Ryan, S.; Fleming, A. Predicted power performance of a submerged membrane pressure-differential wave energy converter. *Int. J. Mar. Energy* **2017**, *20*, 125–134. [CrossRef]

116. Yang, Y.; Zhang, H.; Lee, S.; Kim, D.; Hwang, W.; Wang, Z.L. Hybrid energy cell for degradation of methyl orange by self-powered electrocatalytic oxidation. *Nano Lett.* **2013**, *13*, 803–808. [CrossRef] [PubMed]
117. Iglesias, G.; Carballo, R. Wave farm impact: The role of farm-to-coast distance. *Renew. Energy* **2014**, *69*, 375–385. [CrossRef]
118. Zhao, K.; Gu, G.; Zhang, Y.; Zhang, B.; Yang, F.; Zhao, L.; Zheng, M.; Cheng, G.; Du, Z. The self-powered CO2 gas sensor based on gas discharge induced by triboelectric nanogenerator. *Nano Energy* **2018**, *53*, 898–905. [CrossRef]
119. Liu, X.; Cheng, K.; Cui, P.; Qi, H.; Qin, H.; Gu, G.; Shang, W.; Wang, S.; Cheng, G.; Du, Z. Hybrid energy harvester with bi-functional nano-wrinkled anti-reflective PDMS film for enhancing energies conversion from sunlight and raindrops. *Nano Energy* **2019**, *66*, 104188. [CrossRef]
120. Xi, Y.; Guo, H.; Zi, Y.; Li, X.; Wang, J.; Deng, J.; Li, S.; Hu, C.; Cao, X.; Wang, Z.L. Multifunctional TENG for blue energy scavenging and self-powered wind-speed sensor. *Adv. Energy Mater.* **2017**, *7*, 1602397. [CrossRef]
121. Yoo, D.; Park, S.C.; Lee, S.; Sim, J.Y.; Song, I.; Choi, D.; Lim, H.; Kim, D.S. Biomimetic anti-reflective triboelectric nanogenerator for concurrent harvesting of solar and raindrop energies. *Nano Energy* **2019**, *57*, 424–431. [CrossRef]
122. Yang, X.; Xu, L.; Lin, P.; Zhong, W.; Bai, Y.; Luo, J.; Chen, J.; Wang, Z.L. Macroscopic self-assembly network of encapsulated high-performance triboelectric nanogenerators for water wave energy harvesting. *Nano Energy* **2019**, *60*, 404–412. [CrossRef]
123. Aydoğan, B.; Ayat, B.; Yüksel, Y. Black Sea wave energy atlas from 13 years hindcasted wave data. *Renew. Energy* **2013**, *57*, 436–447. [CrossRef]
124. Calisal, S. A note on the derivation of potential energy for two-dimensional water waves. *Ocean Eng.* **1983**, *10*, 133–138. [CrossRef]
125. Thorpe, T.W. *A Brief Review of Wave Energy*; Harwell Laboratory, Energy Technology Support Unit: London, UK, 1999.
126. Olsen, M.; Zhang, R.; Örtegren, J.; Andersson, H.; Yang, Y.; Olin, H. Frequency and voltage response of a wind-driven fluttering triboelectric nanogenerator. *Sci. Rep.* **2019**, *9*, 1–6. [CrossRef]
127. Suzuki, R.O.; Tanaka, D. Mathematical simulation of thermoelectric power generation with the multi-panels. *J. Power Sources* **2003**, *122*, 201–209. [CrossRef]
128. Prieto, L.F.; Rodríguez, G.R.; Rodríguez, J.S. Wave energy to power a desalination plant in the north of Gran Canaria Island: Wave resource, socioeconomic and environmental assessment. *J. Environ. Manag.* **2019**, *231*, 546–551. [CrossRef]
129. Leijon, M.; Bernhoff, H.; Agren, O.; Isberg, J.; Sundberg, J.; Berg, M.; Karlsson, K.E.; Wolfbrandt, A. Multiphysics simulation of wave energy to electric energy conversion by permanent magnet linear generator. *IEEE Trans. Energy Convers.* **2005**, *20*, 219–224. [CrossRef]
130. Pelc, R.; Fujita, R.M. Renewable energy from the ocean. *Mar. Policy* **2002**, *26*, 471–479. [CrossRef]
131. Chatzigiannakou, M.A.; Dolguntseva, I.; Leijon, M. Offshore deployments of wave energy converters by seabased industry AB. *J. Mar. Sci. Eng.* **2017**, *5*, 15. [CrossRef]
132. Nie, J.; Ren, Z.; Xu, L.; Lin, S.; Zhan, F.; Chen, X.; Wang, Z.L. Probing contact-electrification-induced electron and ion transfers at a liquid–solid interface. *Adv. Mater.* **2020**, *32*, 1905696. [CrossRef] [PubMed]
133. Moskvitch, K. News Briefing: In Num6ers-Sola Road. *Eng. Technol.* **2016**, *11*, 12–13. [CrossRef]
134. Zhao, X.; Chen, B.; Wei, G.; Wu, J.M.; Han, W.; Yang, Y. Polyimide/graphene nanocomposite foam-based wind-driven triboelectric nanogenerator for self-powered pressure sensor. *Adv. Mater. Technol.* **2019**, *4*, 1800723. [CrossRef]
135. McCormick, M.E.; Ertekin, R.C. Renewable sea power. *Mech. Eng.* **2009**, *131*, 36–39. [CrossRef]
136. Deane, J.; Dharmasena, R.; Gentile, G. Power computation for the triboelectric nanogenerator. *Nano Energy* **2018**, *54*, 39–49. [CrossRef]
137. Roscow, J.; Lewis, R.; Taylor, J.; Bowen, C. Corrigendum to "Modelling and fabrication of porous sandwich layer barium titanate with improved piezoelectric energy harvesting figures of merit" [Acta Mater. 128 (2017) 207-217]. *Acta Mater.* **2018**, *152*, 199. [CrossRef]
138. Yousry, Y.M.; Yao, K.; Chen, S.; Liew, W.H.; Ramakrishna, S. Mechanisms for enhancing polarization orientation and piezoelectric parameters of PVDF nanofibers. *Adv. Electron. Mater.* **2018**, *4*, 1700562. [CrossRef]
139. Harstad, S.; D'Souza, N.; Soin, N.; El-Gendy, A.A.; Gupta, S.; Pecharsky, V.K.; Shah, T.; Siores, E.; Hadimani, R.L. Enhancement of β-phase in PVDF films embedded with ferromagnetic Gd5Si4 nanoparticles for piezoelectric energy harvesting. *AIP Adv.* **2017**, *7*, 056411. [CrossRef]
140. Jbaily, A.; Yeung, R.W. Piezoelectric devices for ocean energy: A brief survey. *J. Ocean. Eng. Mar. Energy* **2015**, *1*, 101–118. [CrossRef]
141. Mo, J.; Zhang, C.; Lu, Y.; Liu, Y.; Zhang, N.; Wang, S.; Nie, S. Radial piston triboelectric nanogenerator-enhanced cellulose fiber air filter for self-powered particulate matter removal. *Nano Energy* **2020**, *78*, 105357. [CrossRef]
142. Gu, G.Q.; Han, C.B.; Lu, C.X.; He, C.; Jiang, T.; Gao, Z.L.; Li, C.J.; Wang, Z.L. Triboelectric nanogenerator enhanced nanofiber air filters for efficient particulate matter removal. *ACS Nano* **2017**, *11*, 6211–6217. [CrossRef]
143. Uchino, K. Piezoelectric actuators 2008: Key factors for commercialization. *Adv. Mater. Res.* **2008**, *55*, 1–9. [CrossRef]
144. Marino, A.; Genchi, G.G.; Mattoli, V.; Ciofani, G. Piezoelectric nanotransducers: The future of neural stimulation. *Nano Today* **2017**, *14*, 9–12. [CrossRef]
145. Gao, X.; Wu, J.; Yu, Y.; Chu, Z.; Shi, H.; Dong, S. Giant piezoelectric coefficients in relaxor piezoelectric ceramic PNN-PZT for vibration energy harvesting. *Adv. Funct. Mater.* **2018**, *28*, 1706895. [CrossRef]
146. Damjanovic, D. Ferroelectric, dielectric and piezoelectric properties of ferroelectric thin films and ceramics. *Rep. Prog. Phys.* **1998**, *61*, 1267. [CrossRef]

147. Messing, G.L.; Sabolsky, E.; Kwon, S.; Trolier-McKinstry, S. Templated grain growth of textured piezoelectric ceramics. *Key Eng. Mater.* **2001**, *206*, 1293–1296. [CrossRef]
148. Isarakorn, D.; Sambri, A.; Janphuang, P.; Briand, D.; Gariglio, S.; Triscone, J.M.; Guy, F.; Reiner, J.; Ahn, C.; De Rooij, N. Epitaxial piezoelectric MEMS on silicon. *J. Micromech. Microeng.* **2010**, *20*, 055008. [CrossRef]
149. Muralt, P.; Polcawich, R.G.; Trolier-McKinstry, S. Piezoelectric thin films for sensors, actuators and energy harvesting. *MRS Bull.* **2009**, *34*, 658–664. [CrossRef]
150. Roscow, J.; Taylor, J.; Bowen, C. Manufacture and characterization of porous ferroelectrics for piezoelectric energy harvesting applications. *Ferroelectrics* **2016**, *498*, 40–46. [CrossRef]
151. Martínez-Ayuso, G.; Friswell, M.I.; Adhikari, S.; Khodaparast, H.H.; Berger, H. Homogenization of porous piezoelectric materials. *Int. J. Solids Struct.* **2017**, *113*, 218–229. [CrossRef]
152. Wang, Z.L. Triboelectric nanogenerator (TENG)—Sparking an energy and sensor revolution. *Adv. Energy Mater.* **2020**, *10*, 2000137. [CrossRef]
153. Niu, S.; Wang, Z.L. Theoretical systems of triboelectric nanogenerators. *Nano Energy* **2015**, *14*, 161–192. [CrossRef]
154. Niu, S.; Zhou, Y.S.; Wang, S.; Liu, Y.; Lin, L.; Bando, Y.; Wang, Z.L. Simulation method for optimizing the performance of an integrated triboelectric nanogenerator energy harvesting system. *Nano Energy* **2014**, *8*, 150–156. [CrossRef]
155. Ma, P.; Zhu, H.; Lu, H.; Zeng, Y.; Zheng, N.; Wang, Z.L.; Cao, X. Design of biodegradable wheat-straw based triboelectric nanogenerator as self-powered sensor for wind detection. *Nano Energy* **2021**, *86*, 106032. [CrossRef]
156. Dai, K.; Wang, X.; Niu, S.; Yi, F.; Yin, Y.; Chen, L.; Zhang, Y.; You, Z. Simulation and structure optimization of triboelectric nanogenerators considering the effects of parasitic capacitance. *Nano Res.* **2017**, *10*, 157–171. [CrossRef]
157. Shao, J.; Jiang, T.; Wang, Z. Theoretical foundations of triboelectric nanogenerators (TENGs). *Sci. China Technol. Sci.* **2020**, *63*, 1087–1109. [CrossRef]
158. Shao, J.; Willatzen, M.; Jiang, T.; Tang, W.; Chen, X.; Wang, J.; Wang, Z.L. Quantifying the power output and structural figure-of-merits of triboelectric nanogenerators in a charging system starting from the Maxwell's displacement current. *Nano Energy* **2019**, *59*, 380–389. [CrossRef]
159. Shao, J.; Liu, D.; Willatzen, M.; Wang, Z.L. Three-dimensional modeling of alternating current triboelectric nanogenerator in the linear sliding mode. *Appl. Phys. Rev.* **2020**, *7*, 011405. [CrossRef]
160. Dharmasena, R.D.I.G.; Jayawardena, K.; Mills, C.; Deane, J.; Anguita, J.; Dorey, R.; Silva, S. Triboelectric nanogenerators: Providing a fundamental framework. *Energy Environ. Sci.* **2017**, *10*, 1801–1811. [CrossRef]
161. Dharmasena, R.; Jayawardena, K.; Mills, C.; Dorey, R.; Silva, S. A unified theoretical model for Triboelectric Nanogenerators. *Nano Energy* **2018**, *48*, 391–400. [CrossRef]
162. Shao, J.; Willatzen, M.; Wang, Z.L. Theoretical modeling of triboelectric nanogenerators (TENGs). *J. Appl. Phys.* **2020**, *128*, 111101. [CrossRef]
163. Shao, J.; Willatzen, M.; Shi, Y.; Wang, Z.L. 3D mathematical model of contact-separation and single-electrode mode triboelectric nanogenerators. *Nano Energy* **2019**, *60*, 630–640. [CrossRef]
164. Tang, W.; Jiang, T.; Fan, F.R.; Yu, A.F.; Zhang, C.; Cao, X.; Wang, Z.L. Liquid-metal electrode for high-performance triboelectric nanogenerator at an instantaneous energy conversion efficiency of 70.6%. *Adv. Funct. Mater.* **2015**, *25*, 3718–3725. [CrossRef]
165. Xie, Y.; Wang, S.; Niu, S.; Lin, L.; Jing, Q.; Yang, J.; Wu, Z.; Wang, Z.L. Grating-structured freestanding triboelectric-layer nanogenerator for harvesting mechanical energy at 85% total conversion efficiency. *Adv. Mater.* **2014**, *26*, 6599–6607. [CrossRef] [PubMed]
166. Wang, S.; Niu, S.; Yang, J.; Lin, L.; Wang, Z.L. Quantitative measurements of vibration amplitude using a contact-mode freestanding triboelectric nanogenerator. *ACS Nano* **2014**, *8*, 12004–12013. [CrossRef] [PubMed]
167. Fan, F.R.; Lin, L.; Zhu, G.; Wu, W.; Zhang, R.; Wang, Z.L. Transparent triboelectric nanogenerators and self-powered pressure sensors based on micropatterned plastic films. *Nano Lett.* **2012**, *12*, 3109–3114. [CrossRef] [PubMed]
168. Yang, Y.; Wang, S.; Zhang, Y.; Wang, Z.L. Pyroelectric nanogenerators for driving wireless sensors. *Nano Lett.* **2012**, *12*, 6408–6413. [CrossRef]
169. Zhu, G.; Wang, A.C.; Liu, Y.; Zhou, Y.; Wang, Z.L. Functional electrical stimulation by nanogenerator with 58 V output voltage. *Nano Lett.* **2012**, *12*, 3086–3090. [CrossRef]
170. Yang, Y.; Zhu, G.; Zhang, H.; Chen, J.; Zhong, X.; Lin, Z.H.; Su, Y.; Bai, P.; Wen, X.; Wang, Z.L. Triboelectric nanogenerator for harvesting wind energy and as self-powered wind vector sensor system. *ACS Nano* **2013**, *7*, 9461–9468. [CrossRef]
171. Zhu, G.; Bai, P.; Chen, J.; Wang, Z.L. Power-generating shoe insole based on triboelectric nanogenerators for self-powered consumer electronics. *Nano Energy* **2013**, *2*, 688–692. [CrossRef]
172. Xie, Y.; Wang, S.; Lin, L.; Jing, Q.; Lin, Z.H.; Niu, S.; Wu, Z.; Wang, Z.L. Rotary triboelectric nanogenerator based on a hybridized mechanism for harvesting wind energy. *ACS Nano* **2013**, *7*, 7119–7125. [CrossRef]
173. Zhou, Y.S.; Liu, Y.; Zhu, G.; Lin, Z.H.; Pan, C.; Jing, Q.; Wang, Z.L. In situ quantitative study of nanoscale triboelectrification and patterning. *Nano Lett.* **2013**, *13*, 2771–2776. [CrossRef]
174. Yang, W.; Chen, J.; Zhu, G.; Yang, J.; Bai, P.; Su, Y.; Jing, Q.; Cao, X.; Wang, Z.L. Harvesting energy from the natural vibration of human walking. *ACS Nano* **2013**, *7*, 11317–11324. [CrossRef]
175. Zhu, G.; Chen, J.; Zhang, T.; Jing, Q.; Wang, Z.L. Radial-arrayed rotary electrification for high performance triboelectric generator. *Nat. Commun.* **2014**, *5*, 1–9. [CrossRef]

176. Askari, H.; Khajepour, A.; Khamesee, M.B.; Saadatnia, Z.; Wang, Z.L. Piezoelectric and triboelectric nanogenerators: Trends and impacts. *Nano Today* **2018**, *22*, 10–13. [CrossRef]
177. Jung, Y.; Yu, J.; Hwang, H.J.; Bhatia, D.; Chung, K.B.; Choi, D. Wire-based triboelectric resonator for a self-powered crack monitoring system. *Nano Energy* **2020**, *71*, 104615. [CrossRef]
178. Xu, L.; Jiang, T.; Lin, P.; Shao, J.J.; He, C.; Zhong, W.; Chen, X.Y.; Wang, Z.L. Coupled triboelectric nanogenerator networks for efficient water wave energy harvesting. *ACS Nano* **2018**, *12*, 1849–1858. [CrossRef] [PubMed]
179. Lin, Z.; Zhang, B.; Xie, Y.; Wu, Z.; Yang, J.; Wang, Z.L. Elastic-Connection and Soft-Contact Triboelectric Nanogenerator with Superior Durability and Efficiency. *Adv. Funct. Mater.* **2021**, 2015237.
180. Liang, X.; Liu, Z.; Feng, Y.; Han, J.; Li, L.; An, J.; Chen, P.; Jiang, T.; Wang, Z.L. Spherical triboelectric nanogenerator based on spring-assisted swing structure for effective water wave energy harvesting. *Nano Energy* **2021**, *83*, 105836. [CrossRef]
181. Guan, D.; Cong, X.; Li, J.; Shen, H.; Zhang, C.; Gong, J. Quantitative Characterization of the Energy Harvesting Performance of Soft-contact Sphere Triboelectric Nanogenerator. *Nano Energy* **2021**, *87*, 106186. [CrossRef]
182. Yuan, Z.; Wang, C.; Xi, J.; Han, X.; Li, J.; Han, S.T.; Gao, W.; Pan, C. Spherical Triboelectric Nanogenerator with Dense Point Contacts for Harvesting Multidirectional Water Wave and Vibration Energy. *ACS Energy Lett.* **2021**, *6*, 2809–2816. [CrossRef]
183. Bhatia, D.; Hwang, H.J.; Huynh, N.D.; Lee, S.; Lee, C.; Nam, Y.; Kim, J.G.; Choi, D. Continuous scavenging of broadband vibrations via omnipotent tandem triboelectric nanogenerators with cascade impact structure. *Sci. Rep.* **2019**, *9*, 1–9.
184. Jiang, T.; Yao, Y.; Xu, L.; Zhang, L.; Xiao, T.; Wang, Z.L. Spring-assisted triboelectric nanogenerator for efficiently harvesting water wave energy. *Nano Energy* **2017**, *31*, 560–567. [CrossRef]
185. Xiao, T.X.; Liang, X.; Jiang, T.; Xu, L.; Shao, J.J.; Nie, J.H.; Bai, Y.; Zhong, W.; Wang, Z.L. Spherical triboelectric nanogenerators based on spring-assisted multilayered structure for efficient water wave energy harvesting. *Adv. Funct. Mater.* **2018**, *28*, 1802634. [CrossRef]
186. Wang, W.; Xu, J.; Zheng, H.; Chen, F.; Jenkins, K.; Wu, Y.; Wang, H.; Zhang, W.; Yang, R. A spring-assisted hybrid triboelectric–electromagnetic nanogenerator for harvesting low-frequency vibration energy and creating a self-powered security system. *Nanoscale* **2018**, *10*, 14747–14754. [CrossRef] [PubMed]
187. Wang, S.; Wang, Y.; Liu, D.; Zhang, Z.; Li, W.; Liu, C.; Du, T.; Xiao, X.; Song, L.; Pang, H.; et al. A robust and self-powered tilt sensor based on annular liquid–solid interfacing triboelectric nanogenerator for ship attitude sensing. *Sens. Actuators A Phys.* **2021**, *317*, 112459. [CrossRef]
188. Singh, H.H.; Khare, N. KPFM Study of Flexible Ferroelectric Polymer/Water Interface for Understanding the Working Principle of Liquid–Solid Triboelectric Nanogenerator. *Adv. Mater. Interfaces* **2021**, *8*, 2100032. [CrossRef]
189. Vo, C.P.; Shahriar, M.; Le, C.D.; Ahn, K.K. Mechanically active transducing element based on solid–liquid triboelectric nanogenerator for self-powered sensing. *Int. J. Precis. Eng. Manuf.-Green Technol.* **2019**, *6*, 741–749. [CrossRef]
190. Chung, J.; Cho, H.; Yong, H.; Heo, D.; Rim, Y.S.; Lee, S. Versatile surface for solid–solid/liquid–solid triboelectric nanogenerator based on fluorocarbon liquid infused surfaces. *Sci. Technol. Adv. Mater.* **2020**, *21*, 139–146. [CrossRef]
191. Vu, D.L.; Le, C.D.; Vo, C.P.; Ahn, K.K. Surface polarity tuning through epitaxial growth on polyvinylidene fluoride membranes for enhanced performance of liquid–solid triboelectric nanogenerator. *Compos. Part B Eng.* **2021**, *223*, 109135. [CrossRef]
192. Xu, M.; Wang, S.; Zhang, S.L.; Ding, W.; Kien, P.T.; Wang, C.; Li, Z.; Pan, X.; Wang, Z.L. A highly-sensitive wave sensor based on liquid–solid interfacing triboelectric nanogenerator for smart marine equipment. *Nano Energy* **2019**, *57*, 574–580. [CrossRef]
193. Wei, X.; Zhao, Z.; Zhang, C.; Yuan, W.; Wu, Z.; Wang, J.; Wang, Z.L. All-Weather Droplet-Based Triboelectric Nanogenerator for Wave Energy Harvesting. *ACS Nano* **2021**, online ahead of print. [CrossRef]
194. Nie, J.; Jiang, T.; Shao, J.; Ren, Z.; Bai, Y.; Iwamoto, M.; Chen, X.; Wang, Z.L. Motion behavior of water droplets driven by triboelectric nanogenerator. *Appl. Phys. Lett.* **2018**, *112*, 183701. [CrossRef]
195. Jung, W.S.; Kang, M.G.; Moon, H.G.; Baek, S.H.; Yoon, S.J.; Wang, Z.L.; Kim, S.W.; Kang, C.Y. High output piezo/triboelectric hybrid generator. *Sci. Rep.* **2015**, *5*, 1–6. [CrossRef]
196. Chen, X.; Han, M.; Chen, H.; Cheng, X.; Song, Y.; Su, Z.; Jiang, Y.; Zhang, H. A wave-shaped hybrid piezoelectric and triboelectric nanogenerator based on P (VDF-TrFE) nanofibers. *Nanoscale* **2017**, *9*, 1263–1270. [CrossRef]
197. He, W.; Qian, Y.; Lee, B.S.; Zhang, F.; Rasheed, A.; Jung, J.E.; Kang, D.J. Ultrahigh output piezoelectric and triboelectric hybrid nanogenerators based on ZnO nanoflakes/polydimethylsiloxane composite films. *ACS Appl. Mater. Interfaces* **2018**, *10*, 44415–44420. [CrossRef] [PubMed]
198. Li, Z.; Saadatnia, Z.; Yang, Z.; Naguib, H. A hybrid piezoelectric-triboelectric generator for low-frequency and broad-bandwidth energy harvesting. *Energy Convers. Manag.* **2018**, *174*, 188–197. [CrossRef]
199. Yang, D.; Ni, Y.; Su, H.; Shi, Y.; Liu, Q.; Chen, X.; He, D. Hybrid energy system based on solar cell and self-healing/self-cleaning triboelectric nanogenerator. *Nano Energy* **2021**, *79*, 105394. [CrossRef]
200. Gao, L.; Lu, S.; Xie, W.; Chen, X.; Wu, L.; Wang, T.; Wang, A.; Yue, C.; Tong, D.; Lei, W.; et al. A self-powered and self-functional tracking system based on triboelectric-electromagnetic hybridized blue energy harvesting module. *Nano Energy* **2020**, *72*, 104684. [CrossRef]
201. Wu, Z.; Guo, H.; Ding, W.; Wang, Y.C.; Zhang, L.; Wang, Z.L. A hybridized triboelectric–electromagnetic water wave energy harvester based on a magnetic sphere. *ACS Nano* **2019**, *13*, 2349–2356. [CrossRef]
202. Wang, P.; Liu, R.; Ding, W.; Zhang, P.; Pan, L.; Dai, G.; Zou, H.; Dong, K.; Xu, C.; Wang, Z.L. Complementary electromagnetic-triboelectric active sensor for detecting multiple mechanical triggering. *Adv. Funct. Mater.* **2018**, *28*, 1705808. [CrossRef]

203. Wang, P.; Pan, L.; Wang, J.; Xu, M.; Dai, G.; Zou, H.; Dong, K.; Wang, Z.L. An ultra-low-friction triboelectric–electromagnetic hybrid nanogenerator for rotation energy harvesting and self-powered wind speed sensor. *ACS Nano* **2018**, *12*, 9433–9440. [CrossRef]
204. Hao, C.; He, J.; Zhang, Z.; Yuan, Y.; Chou, X.; Xue, C. A pendulum hybrid generator for water wave energy harvesting and hydrophone-based wireless sensing. *AIP Adv.* **2020**, *10*, 125019. [CrossRef]
205. He, J.; Fan, X.; Mu, J.; Wang, C.; Qian, J.; Li, X.; Hou, X.; Geng, W.; Wang, X.; Chou, X. 3D full-space triboelectric-electromagnetic hybrid nanogenerator for high-efficient mechanical energy harvesting in vibration system. *Energy* **2020**, *194*, 116871. [CrossRef]
206. Wu, Z.; Ding, W.; Dai, Y.; Dong, K.; Wu, C.; Zhang, L.; Lin, Z.; Cheng, J.; Wang, Z.L. Self-powered multifunctional motion sensor enabled by magnetic-regulated triboelectric nanogenerator. *ACS Nano* **2018**, *12*, 5726–5733. [CrossRef] [PubMed]
207. Huang, L.b.; Xu, W.; Bai, G.; Wong, M.C.; Yang, Z.; Hao, J. Wind energy and blue energy harvesting based on magnetic-assisted noncontact triboelectric nanogenerator. *Nano Energy* **2016**, *30*, 36–42. [CrossRef]
208. Seol, M.L.; Han, J.W.; Jeon, S.B.; Meyyappan, M.; Choi, Y.K. Floating oscillator-embedded triboelectric generator for versatile mechanical energy harvesting. *Sci. Rep.* **2015**, *5*, 1–10. [CrossRef]
209. Liu, S.; Li, X.; Wang, Y.; Yang, Y.; Meng, L.; Cheng, T.; Wang, Z.L. Magnetic switch structured triboelectric nanogenerator for continuous and regular harvesting of wind energy. *Nano Energy* **2021**, *83*, 105851. [CrossRef]
210. Wu, Z.; Zhang, B.; Zou, H.; Lin, Z.; Liu, G.; Wang, Z.L. Multifunctional sensor based on translational-rotary triboelectric nanogenerator. *Adv. Energy Mater.* **2019**, *9*, 1901124. [CrossRef]
211. Liu, G.; Chen, J.; Guo, H.; Lai, M.; Pu, X.; Wang, X.; Hu, C. Triboelectric nanogenerator based on magnetically induced retractable spring steel tapes for efficient energy harvesting of large amplitude motion. *Nano Res.* **2018**, *11*, 633–641. [CrossRef]